Vernalization-triggered expression of the antisense transcript *COOLAIR* is mediated by *CBF* genes

Myeongjune Jeon[1,2†], Goowon Jeong[1,2†], Yupeng Yang[3], Xiao Luo[4], Daesong Jeong[1,2], Jinseul Kyung[1,2], Youbong Hyun[1,2], Yuehui He[3,4,*], and Ilha Lee[1,2,*]

[1] School of Biological Sciences, Seoul National University, Seoul 08826, Korea
[2] Research Center for Plant Plasticity, Seoul National University, Seoul 08826, Korea
[3] Shanghai Center for Plant Stress Biology & National Key Laboratory for Plant Molecular Genetics, CAS Center for Excellence in Molecular Plant Sciences, Chinese Academy of Sciences (CAS), Shanghai 201602, China
[4] Peking University Institute of Advanced Agricultural Sciences, Weifang 261325, China

[*] For correspondence: ilhalee@snu.ac.kr, yhhe@pku.edu.cn
[†] These authors contributed equally to this work.

Abstract

To synchronize flowering time with spring, many plants undergo vernalization, a floral-promotion process triggered by exposure to long-term winter cold. In *Arabidopsis thaliana*, this is achieved through cold-mediated epigenetic silencing of the floral repressor, *FLOWERING LOCUS C* (*FLC*). *COOLAIR*, a cold-induced antisense RNA transcribed from the *FLC* locus, has been proposed to facilitate *FLC* silencing. Here, we show that C-repeat (CRT)/dehydration-responsive elements (DREs) at the 3′-end of *FLC* and CRT/DRE-binding factors (CBFs) are required for cold-mediated expression of *COOLAIR*. CBFs bind to CRT/DREs at the 3′-end of *FLC*, both *in vitro* and *in vivo*, and CBF levels increase gradually during vernalization. Cold-induced *COOLAIR* expression is severely impaired in *cbfs* mutants in which all *CBF* genes are knocked-out. Conversely, *CBF*-overexpressing plants show increased *COOLAIR* levels even at warm temperatures. We show that *COOLAIR* is induced by CBFs during early stages of vernalization but COOLAIR levels decrease in later phases as *FLC* chromatin transitions to an inactive state to which CBFs can no longer bind. We also demonstrate that *cbfs* and $FLC_{\Delta COOLAIR}$ mutants exhibit a normal vernalization response despite their inability to activate *COOLAIR* expression during cold, revealing that *COOLAIR* is not required for the vernalization process.

Introduction

Appropriate timing of flowering provides evolutionary advantage of plant reproductive success. As sessile organisms, plants have evolved mechanisms through which seasonal cues coordinate the transition to flowering. One of the significant environmental factors affecting flowering time of plants adapted to temperate climates is the temperature changes during the seasons, and plants have evolved complex sensory mechanisms to monitor the surrounding temperature to properly control the timing of flowering and tolerate thermal stress (*Went, 1953; Penfield, 2008; Ding and Yang, 2022*).

Cold acclimation and vernalization are two responses of plants to low temperatures. Cold acclimation is generally initiated by a short period of non-freezing cold exposure and increases the frost tolerance of plants (*Weiser, 1970; Gilmour et al., 1988; Guy, 1990; Thomashow, 1999; Chinnusamy et al., 2007*). The three C-REPEAT(CRT)/DEHYDRATION-RESPONSIVE ELEMENT (DRE) BINDING FACTORs (CBFs) and their encoding genes serve as signaling hubs for cold acclimation in *Arabidopsis thaliana* (*Stockinger et al., 1997; Medina et al., 1999; Thomashow, 2010; Ding et al., 2019*). When exposed to low temperatures, the transcription of *CBFs* is rapidly promoted by a group of cold-signal transducers, including the Ca^{2+}/calmodulin-binding proteins, CALMODULIN-BINDING TRANSCRIPTION ACTIVATORs (CAMTAs) (*Doherty et al., 2009; Kim et al., 2013; Kidokoro et al., 2017*); the clock proteins, CIRCADIAN CLOCK-ASSOCIATED 1 (CCA1) and LATE-ELONGATED HYPOCOTYL (LHY) (*Dong et al., 2011*); and the brassinosteroid-responsive proteins, BRASSINAZOLE-RESISTANT 1 (BZR1) and CESTA (CES) (*Eremina et al., 2016; Li et al., 2017*). In addition, cold also enhances the

activity of CBF proteins by triggering degradation of BASIC TRANSCRIPTION FACTOR 3s (BTF3s) and HISTONE DEACETYLASE 2C (HD2C) which prevent CBFs from activating their targets (*Ding et al., 2018; J. Park et al., 2018*), or by reducing oxidized CBFs, which increases active CBF monomers (*Lee et al., 2021*). Low temperature-induced CBFs, in turn, activate the expression of *co*ld-*r*egulated (*COR*) genes by binding to CRT/DREs in their promoters (*Stockinger et al., 1997; Medina et al., 1999*). Diverse arrays of cryoprotective proteins encoded by *COR* genes allow plants to overcome freezing stress (*Gilmour et al., 1988; Hajela et al., 1990; Thomashow et al., 1997; Shinozaki et al., 2003; Shi et al., 2018; Ding et al., 2019*).

In contrast to cold acclimation, vernalization, a floral-promotion process that occurs during winter, requires an extended cold period (*Napp-Zinn, 1955; Chouard, 1960; Michaels and Amasino, 2000*). This allows plants to synchronize the timing of flowering with favorable spring conditions. Vernalization in *A. thaliana* is mainly achieved by silencing the floral repressor gene, *FLOWERING LOCUS C* (*FLC*) (*Michaels and Amasino, 1999; Sheldon et al., 1999; Sheldon et al., 2000; Michaels and Amasino, 2001*). *FLC* encodes a MADS-box protein that represses the expression of floral activator genes, *SUPPRESSOR OF OVEREXPRESSION OF CO 1* (*SOC1*) and *FLOWERING LOCUS T* (*FT,* encoding florigen), by directly binding to their promoter regions (*Lee et al., 2000; Michaels et al., 2005; Helliwell et al., 2006*). In Arabidopsis winter annuals, such as San Feliu-2, Löv-1, and Sweden (SW) ecotypes, flowering is prevented by the high expression of *FLC* before exposure to winter cold (*Lee et al., 1993; Shindo et al., 2005; S. Park et al., 2018*). This is caused by the strong transcriptional activation of *FLC* by the FRIGIDA (FRI) supercomplex, which recruits general transcription factors and several chromatin modifiers (*Michaels and Amasino, 1999; Sheldon et al., 1999; Johanson et al., 2000; Choi et al., 2011; Li et al., 2018*).

77 Prior to vernalization, *FLC* chromatin is highly enriched with active histone marks such as histone
78 H3 acetylation and trimethylation of Lys4 or Lys36 at H3 (H3K4me3/H3K36me3) (*Bastow et al.,*
79 *2004; Yang et al., 2014*). In contrast, prolonged cold exposure results in gradual deacetylation of
80 *FLC* chromatin and concomitant removal of H3K4me3 and H3K36me3 from the *FLC* (*Bastow et*
81 *al., 2004; Yang et al., 2014; Nishio et al., 2016*). Additionally, VP1/ABI3-LIKE 1 (VAL1) and
82 VAL2 recruit Polycomb Repressive Complex 2 (PRC2) onto *FLC* chromatin, thereby
83 accumulating the repressive histone mark, H3 Lys27 trimethylation (H3K27me3), in the nucleation
84 region around the first exon and intron of *FLC* (*Sung and Amasino, 2004b; Wood et al., 2006; De*
85 *Lucia et al., 2008; Angel et al., 2011; Nishio et al., 2016; Qüesta et al., 2016; Yuan et al., 2016*).
86 Subsequently, upon returning to warm temperatures, H3K27me3 marks are spread over the entire
87 *FLC* chromatin region by LIKE HETEROCHROMATIN PROTEIN 1 (LHP1), which ensures
88 stable *FLC* suppression and renders plants competent to flower (*Mylne et al., 2006; Sung et al.,*
89 *2006; Yang et al., 2017*).

90 Several long-term cold-induced factors have been shown to play crucial roles in the epigenetic
91 silencing of *FLC*. *VERNALIZATION INSENSITIVE 3* (*VIN3*) family genes, which are upregulated
92 by prolonged cold, encode plant homeodomain (PHD) proteins that recognize H3K9me2 enriched
93 in *FLC* chromatin during vernalization (*Sung and Amasino, 2004b; Kim and Sung, 2013*, *2017a*).
94 These proteins mediate the recruitment of PRC2 and the subsequent deposition of H3K27me3 at
95 the *FLC* nucleation region (*Sung and Amasino, 2004b; De Lucia et al., 2008; Kim and Sung, 2013*).
96 In addition, vernalization-induced long non-coding RNAs (lncRNAs) are involved in such histone
97 modifications. *COLDAIR* and *COLDWRAP*, the two lncRNAs transcribed from the first intron and
98 promoter region of *FLC*, respectively, are required for H3K27me3 deposition in response to long-

99 term cold (*Heo and Sung, 2011; Kim and Sung, 2017b*). *COLDAIR* and *COLDWRAP* are also
100 thought to affect the formation of the intragenic chromatin loop at the *FLC*, which may be a part
101 of the *FLC* silencing mechanism (*Kim and Sung, 2017b*). Unlike *COLDAIR* and *COLDWRAP*,
102 which are transcribed in the sense direction of *FLC*, another lncRNA, *COOLAIR,* is an antisense
103 transcript expressed from the 3′-end of *FLC* (*Swiezewski et al., 2009*). The gradual accumulation
104 of *COOLAIR* reaches a maximum within a few weeks of cold exposure, whereas *COLDAIR* and
105 *COLDWRAP* showed peaks at a later phase of vernalization (*Csorba et al., 2014; Kim and Sung,*
106 *2017b*). *COOLAIR* was reported to remove active histone marks from *FLC* chromatin (*Liu et al.,*
107 *2007; Csorba et al., 2014; Fang et al., 2020; Xu, Fang, et al., 2021; Zhu et al., 2021*). Particularly,
108 in summer annuals, phase-separated RNA-processing complexes favor co-transcriptional proximal
109 polyadenylation of *COOLAIR* (*Marquardt et al., 2014; Wang et al., 2014; Fang et al., 2019; Wu*
110 *et al., 2020; Xu, Wu, et al., 2021*). The *COOLAIR*-processing machinery exhibits transient and
111 dynamic interactions with an H3K4 demethylation complex, leading to *FLC* suppression at warm
112 temperatures (*Liu et al., 2007; Fang et al., 2020; Xu, Fang, et al., 2021*). *COOLAIR* is also likely
113 to be involved in reducing H3K36me3 at the *FLC* during vernalization process (*Csorba et al.,*
114 *2014*). *COOLAIR* was reported to promote the sequestration of the FRI complex from the *FLC*
115 promoter by condensing it into phase-separated nuclear bodies (*Zhu et al., 2021*). This has been
116 suggested to cause the inactivation of *FLC,* which is probably accompanied by the silencing of
117 *FLC* chromatin through the removal of H3K36me3. However, a previous study has raised the issue
118 that *COOLAIR* appears not to be necessary for vernalization (*Helliwell et al., 2011; Luo et al.,*
119 *2019*).

120 Compared with the signaling pathway of cold acclimation, how a long-term cold signal is

121 transduced to trigger the induction of *VIN3* and lncRNAs is less well understood. It is marginally
122 known that some chromatin modifiers, NAC WITH TRANSMEMBRANE MOTIF 1-LIKE 8
123 (NTL8), and CCA1/LHY act as positive regulators of *VIN3* during the vernalization process (*Kim*
124 *et al., 2010; Finnegan et al., 2011; Zhao et al., 2020; Kyung et al., 2022*). However, little is known
125 about the upstream regulators of *COOLAIR* required for cold-induction. Recent reports have
126 shown that an NAC domain-containing protein, NTL8, and the WRKY transcription factor,
127 WRKY63, can bind to the promoter of *COOLAIR* and activate its expression (*Zhao et al., 2021;*
128 *Hung et al., 2022*). However, whether NTL8 and WRKY63 are necessary for the full extent of
129 *COOLAIR* induction during vernalization has not been thoroughly addressed. In this study, we
130 identified that CRT/DREs at the 3′-end of the *FLC* are required for the long-term cold response of
131 *COOLAIR*. Additionally, we show that CBFs, which accumulate during the long-term winter cold,
132 act as upstream regulators of *COOLAIR* during vernalization.

133 # Results

134

135 **A CRT/DRE-binding factor, CBF3, directly binds to CRT/DREs at the 3′-end of the *FLC***

136 The proximal promoter region of *COOLAIR* is highly conserved among *FLC* orthologs from *A.*
137 *thaliana* relatives (*Castaings et al., 2014*). Thus, we assumed that the cis-element conferring a
138 long-term cold response would exist within that block. A comparison of the region near the
139 transcriptional start site (TSS) of *COOLAIR* revealed the conservation of two CRT/DREs among
140 six *FLC* orthologs from five related species of the Brassicaceae family (***Figure 1A***). CRT/DRE,
141 the core sequence of which is CCGAC, is a regulatory element that imparts cold- or drought-
142 responsive gene expression (*Baker et al., 1994*). *CBF1*, *2*, and *3* encode APETALA2 (AP2)
143 domain-containing proteins that can bind to CRT/DRE and are usually present in the promoters of
144 cold- and drought-responsive genes (*Stockinger et al., 1997; Medina et al., 1999*). Consistent with
145 this, the Arabidopsis cistrome database and the genome-wide chromatin immunoprecipitation
146 sequencing (ChIP-seq) results from a previous study suggested that CBFs bind to the 3′-end
147 sequence of *FLC* containing CRT/DREs (***Figure 1—figure supplement 1***; *O'Malley et al., 2016;*
148 *Song et al., 2021*).

149 We performed an electrophoretic mobility shift assay (EMSA) to confirm this binding using
150 probes harboring CRT/DREs (named DRE1 or 2) from the *COOLAIR* promoter. The mobility of
151 these two Cy5-labeled probes was retarded by maltose-binding protein (MBP)-fused CBF3
152 (***Figure 1B, Figure 1—figure supplement 2***). The band shift was competed out by adding an
153 excess amount of unlabeled DRE1 or 2 oligonucleotides. In contrast, competitors containing
154 mutant forms of DRE1 or 2 ($DRE1^m$ or 2^m, respectively) failed to compete (***Figure 1B***). We also

155 tested the binding of other CRT/DRE-like sequences in the *FLC* locus. Two (DREa and b) were
156 present in the *FLC* promoter, while the other two (DREc and d), were present in the first and last
157 exons, respectively (***Figure 1—figure supplement 2***). Only DREc competed with the band shift
158 caused by the CBF3-DRE1 interaction (***Figure 1B, Figure 1—figure supplement 2***). The presence
159 or absence of bases that determine the binding affinity between CBFs and CRT/DRE could explain
160 the differences in CBF3-binding patterns among CRT/DRE-like sequences at the *FLC* locus
161 (*Maruyama et al., 2004*).

162 Subsequently, a chromatin immunoprecipitation (ChIP) assay using a *CBF3*-overexpressing
163 transgenic plant, *pSuper:CBF3-myc* (*Liu et al., 2017*), was conducted to determine whether CBF3
164 is associated with the *FLC* region containing CRT/DREs *in vivo*. Consistent with the *in vitro* results,
165 CBF3-myc protein was enriched at the 3′-end of *FLC* and the first exon where DREc was located
166 (***Figure 1C***). Without vernalization (NV), CBF3-myc was highly enriched at both the 5′- and 3′-
167 ends of *FLC* (P1 and P3), indicating that CBF3 protein can activate *FLC* under warm conditions,
168 as previously reported (*Seo et al., 2009*). However, enrichment in the P1 region rapidly disappeared
169 during the vernalization period. In contrast, enrichment on P3 was maintained until 10 days of
170 vernalization (10V) and was subsequently reduced. This is coincident with the expression pattern
171 of *COOLAIR*, which declines during the late phase of vernalization (*Csorba et al., 2014*).

172

173 **_COOLAIR_ is one of the CBF regulons in Arabidopsis**

174 *CBF* genes are rapidly and transiently induced upon exposure to cold (*Medina et al., 1999*). CBF
175 regulons, which are CBF-targeted genes, are correspondingly up- or down-regulated after cold
176 intervals of a few hours (*Gilmour et al., 1998; Liu et al., 1998; Fowler and Thomashow, 2002*).

177 As *COOLAIR* contains CBF3-binding sites in its promoter (***Figure 1***), we analyzed whether
178 *COOLAIR* shows CBF regulon-like expression. The expression of genes assigned to the CBF
179 regulon is up- or down-regulated by *CBF* overexpression under warm conditions (*Park et al.,*
180 *2015*). Similarly, we found that the total transcript level of *COOLAIR* increased in *CBF3*-
181 overexpressing transgenic plants (*pSuper:CBF3-myc*) grown at room temperature (22°C)
182 compared to that in the wild type, Columbia-0 (Col-0) (***Figure 2A***). Such upregulation was mainly
183 due to the type I.i or type II.i *COOLAIR* isoforms. As the levels of both proximal (type I) and distal
184 (type II) variants of *COOLAIR* were higher in the *CBF3* overexpressor than in the wild type, it is
185 likely that *COOLAIR* transcription, instead of the 3′-processing events, is affected by CBF3
186 (***Figure 2A;*** *Liu et al., 2010; Marquardt et al., 2014*). It has been reported that the targets of CBF1
187 or 2 are not entirely identical to those of CBF3, although *CBF* genes show high sequence similarity
188 (*Novillo et al., 2007*). Thus, we compared the expression levels of all *COOLAIR* isoforms in
189 transgenic plants overexpressing *CBF1*, *2*, or *3* (*Seo et al., 2009*). Overall, all CBF-overexpressing
190 plants showed increased levels of *COOLAIR* (***Figure 2—figure supplement 1***). However, each
191 *CBF*-overexpressing plant showed a subtly different effect on *COOLAIR* expression. The *CBF2*
192 overexpressor showed the highest level of the proximal *COOLAIR* isoform, whereas the *CBF3*
193 overexpressor showed the highest level of distal *COOLAIR*. In contrast, the *CBF1*-overexpressing
194 plants showed a slightly smaller increase in proximal *COOLAIR* levels and a negligible increase
195 in distal *COOLAIR*, compared to those in the wild type, Wassilewskija-2 (Ws-2). Such results
196 imply that the three CBFs regulate *COOLAIR* transcription subtly differently.

197 Another characteristic of CBF regulons is that their expression is activated by a day of cold
198 exposure (*Park et al., 2015*). Thus, we analyzed if *COOLAIR* is also induced by short-term cold

199 exposure. We treated wild-type (*FRI* Col) plants with 0, 0.5, 1, 1.5, 2, 3, 6, and 24 h of cold (4°C),
200 then measured the levels of total *COOLAIR*. The results showed that cold treatment for less than
201 3 h failed to induce *COOLAIR* expression, although *CBF* transcripts reached a peak at 3 h of cold
202 exposure (***Figures 2B and 3A;*** *Gilmour et al., 1998*). However, after 6 h of cold treatment, when
203 CBF3 protein levels peaked, *COOLAIR* was strongly induced (***Figures 2B and 3D***). Thus, short-
204 term cold-triggered *COOLAIR* expression dynamics were similar to those of other CBF-targeted
205 genes; that is, the expression was highly increased after *CBF* transcript levels reached a peak upon
206 cold exposure (*Gilmour et al., 1998; Fowler and Thomashow, 2002*). To confirm whether *CBFs*
207 are responsible for the rapid cold response of *COOLAIR*, we examined *COOLAIR* induction after
208 a day of cold treatment in the wild type and *cbfs-1* mutant, in which all three *CBFs* were knocked
209 out (***Figure 2C;*** *Jia et al., 2016*). All isoforms, as well as total *COOLAIR*, failed to be induced by
210 short-term cold exposure in the *cbfs* mutant, although a drastic increase was observed in the wild
211 type. Thus, these results strongly suggest that *CBFs* are required for *COOLAIR* induction, even
212 under a short period of cold exposure.
213

214 **CBFs accumulate during vernalization**

215 We subsequently investigated whether *CBFs* are also responsible for vernalization-induced
216 *COOLAIR* activation. It has been reported that *COOLAIR* is gradually upregulated as the cold
217 period persists and peaks after 2–3 weeks of vernalization (*Csorba et al., 2014*). However, most
218 studies on *CBF* expression have been performed within a few days since the function of *CBFs* has
219 been analyzed only in the context of short-term cold (*Gilmour et al., 1998; Liu et al., 1998; Medina*
220 *et al., 1999; McKhann et al., 2008*). Therefore, we investigated the expression patterns of *CBFs*

221 before and after long-term cold exposure to determine the correlation between the expression of
222 *CBFs* and *COOLAIR* during vernalization. As previously shown, the levels of all three *CBFs*
223 peaked within 3 h of cold exposure and then decreased rapidly (***Figure 3A***). However, *CBF* levels
224 increased again as the cold period was prolonged (> 20V), suggesting that both short-term and
225 vernalizing cold treatments upregulated *CBF* expression (***Figure 3B***).

226 Because *CBFs* exhibit rhythmic oscillations (*Dong et al., 2011*), we also investigated whether
227 the rhythmic expression of *CBFs* is affected by vernalization. Wild-type (Col-0) plants were
228 collected every 4 h under a short-day cycle (SD, 8 h light/16 h dark) under both NV and 40V
229 conditions. As shown in ***Figure 3C***, although the rhythmic pattern of each *CBF* was variable, the
230 overall transcript levels of all three *CBFs* were much higher at 40V than under NV. Consistent with
231 the transcript level, the level of CBF3 protein in vernalized plants was higher than that in NV
232 plants during all circadian cycles (***Figure 3—figure supplement 1***).

233 To verify whether the increased transcription of *CBF3* led to protein accumulation, we
234 measured the level of CBF3 at each time-point of cold treatment using the *pCBF3:CBF3-myc* plant
235 (*Jia et al., 2016*). Following the rapid and transient induction of *CBF3* under short-term cold
236 conditions (***Figure 3A;*** *Medina et al., 1999*), CBF3-myc protein levels peaked within 6 h of cold
237 exposure and then decreased (***Figure 3D***). Thus, the peak of the *CBF3* transcript and that of the
238 CBF3 protein showed a gap of few hours. Notably, the peak of the CBF3 protein correlated with
239 the time when *COOLAIR* was rapidly induced (***Figures 2B and 3D***). During vernalization, the
240 level of CBF3-myc protein gradually declined until 10V, but then increased again (***Figure 3E***).
241 Thus, the level at 40V is similar to that at 1V. When the plants were transferred to room temperature
242 for 4 d after 40V (40VT4), the protein level rapidly decreased. These results suggest that CBFs are

243 responsible for the progressive upregulation of *COOLAIR*, at least during the early phase of
244 vernalization (*Csorba et al., 2014*).
245
246 **_CBFs_ are involved in vernalization-induced _COOLAIR_ expression**
247 To clarify whether *CBFs* are responsible for long-term cold-mediated *COOLAIR* induction, we
248 quantified *COOLAIR* levels in wild type and *cbfs* mutant during vernalization. As shown in
249 ***Figures 2B and 2C***, the *COOLAIR* level was considerably increased by a day of low-temperature
250 treatment in the wild type but quickly declined afterward (***Figure 4A***). The *COOLAIR* level
251 increased again after 4V and reached a secondary peak at approximately 10V to 20V. It then
252 decreased during the remaining vernalization period, as similar to previous results (*Csorba et al.,*
253 *2014*). The expression dynamics of *COOLAIR* were similar to those of two well-known CBF
254 targets, *COR15A* and *RD29A*, although their levels remained high until the end of the vernalization
255 period (***Figure 4—figure supplement 1***). In contrast to the wild type plants, the *cbfs* mutant
256 showed severely reduced *COOLAIR* expression, as well as *COR15A* and *RD29A* levels, during all
257 the period of vernalization (***Figure 4A, Figure 4—figure supplement 1***). Analysis of RNA
258 sequencing (RNA-seq) data from previous studies also revealed that the levels of total *COOLAIR,*
259 and proximal and distal *COOLAIR* variants were reduced in the *cbfs* mutant in Col-0 or SW
260 ecotype background when exposed to either short-term (3 and 24 h) or long-term (14V) cold, which
261 supports our results (***Figure 4—figure supplement 2;*** *Zhao et al., 2016; S. Park et al., 2018*). All
262 of these data support that *CBFs* are necessary to fully induce *COOLAIR* in the early phase of
263 vernalization.
264 Consistent with the reduced *COOLAIR* levels in *cbfs* mutants, the *CBF3* overexpressor,

265 *pSuper:CBF3-myc*, showed a much higher *COOLAIR* level than the wild type (Col-0), throughout
266 the vernalization period (***Figure 4B***). It is noteworthy that *COOLAIR* expression in *pSuper:CBF3-*
267 *myc* was further upregulated by cold, especially during the early vernalization phase (10V), and
268 then suppressed during the late phase. This result implies that both the transcriptional and post-
269 transcriptional regulations of CBFs are involved in the long-term cold response of *COOLAIR*.

270 A recent study showed that the first seasonal frost (< 0°C) during the winter season strongly
271 induces *COOLAIR* expression (*Zhao et al., 2021*). Therefore, we tested whether *CBFs* are also
272 required for the strong induction of *COOLAIR* triggered by freezing temperatures. Wild-type and
273 *cbfs* plants were subjected to NV, 10V, and 20V, with or without an additional 8 h of −1°C freezing
274 treatment. Irrespective of the pre-treatment with non-freezing cold, the freezing temperature
275 increased the levels of both *COOLAIR* and *CBF* in the wild type (***Figure 4C, Figure 4—figure***
276 ***supplement 3***). However, the *cbfs* mutants showed a much smaller increase in the *COOLAIR* level
277 than the wild type when exposed to 8 h of sub-zero cold after 10V and 20V (***Figure 4C***). In
278 particular, *COOLAIR* levels were not elevated by freezing treatment in NV *cbfs*. Thus, *CBFs* seem
279 responsible for both the gradual increase of *COOLAIR* during vernalization and the strong
280 *COOLAIR* induction triggered by freezing temperatures.

281

282 **CRT/DREs at the 3′-end of *FLC* are necessary for CBFs-mediated induction of *COOLAIR***
283 **during vernalization.**

284 Since CBF3 could bind to the CRT/DREs in the first exon (DREc) and the 3′-end of *FLC* (DRE1
285 and 2) (***Figures 1B and 1C***), we investigated whether CRT/DRE is responsible for the CBF-
286 mediated long-term cold response of *COOLAIR*. To address this, we performed an *A. thaliana*

287 protoplast transfection assay using the *35S:CBF3-HA* effector construct and the
288 *pCOOLAIR*$_{DRE}$*:LUC* reporter construct, in which the 1-kb wild-type *COOLAIR* promoter was
289 fused to the luciferase reporter gene. The luciferase activity assay showed that CBF3-HA protein
290 activated the transcription of the *COOLAIR* promoter (***Figure 5A***). In contrast, CBF3-HA failed
291 to increase luciferase activity when the mutant version of the *COOLAIR* promoter with mutations
292 in the DRE1 and 2 sequences (*pCOOLAIR*$_{DRE}^{m}$*:LUC*) was used as a reporter. Additionally, co-
293 transfection of the *35S:CBF3-HA* effector and *pFLC:LUC* reporter construct, which harbors the
294 1-kb sequence with the promoter and first exon of *FLC*, did not show increased luciferase activity.
295 These results strongly indicate that CBF3 can activate *COOLAIR* transcription through DRE1 and
296 2 located in the *COOLAIR* promoter, but not *via* the first exon of *FLC*.

297 To further determine whether the 3′-end sequence of *FLC* is required for cold-induction of
298 *COOLAIR* expression, we measured *COOLAIR* expression before and after vernalization in the
299 *FLC*$_{\Delta COOLAIR}$ mutant (*FLC*$_{\Delta COOLAIR\text{-}1}$), that lacks a 324-bp portion of the *COOLAIR* promoter region
300 (*Luo et al., 2019*). Reverse transcription PCR (RT-PCR) analysis showed that neither proximal nor
301 distal *COOLAIR* variants were detected in this mutant, and the levels did not increase after 14-d
302 cold exposure (***Figure 5B***). Using the CRISPR-Cas9 system, we generated additional *FLC*$_{\Delta COOLAIR}$
303 mutant lines, *FLC*$_{\Delta COOLAIR\text{-}3}$, and *FLC*$_{\Delta COOLAIR\text{-}4}$ (***Figure 5B; Figure 5—figure supplement 1***).
304 *FLC*$_{\Delta COOLAIR\text{-}3}$ has a 685-bp deletion in the *COOLAIR* promoter region where both CRT/DREs are
305 located. As expected, this mutant failed to express *COOLAIR* even after 14V, which is similar to
306 the *FLC*$_{\Delta COOLAIR\text{-}1}$ mutant. In contrast, the *FLC*$_{\Delta COOLAIR\text{-}4}$ mutant, which bears a 301-bp deletion in
307 the distal *COOLAIR* promoter region (upstream of CRT/DREs) and a 13-bp sequence replacement
308 downstream of CRT/DREs, showed a normal vernalization-induced increase in all *COOLAIR*

309 variants, similar to the wild type. This strongly suggests that CRT/DREs located at the *COOLAIR*
310 promoter are critical for CBF-mediated *COOLAIR* induction during vernalization. Notably, the
311 low-abundance convergent antisense transcripts (*CAS*; *Zhao et al., 2021*) were similarly reduced
312 by 14V in all genotypes, i.e., the wild type and $FLC_{\Delta COOLAIR}$ mutants (***Figure 5B***), suggesting their
313 regulation is independent of *COOLAIR*.

314 Although the common *COOLAIR* TSS was eliminated in $FLC_{\Delta COOLAIR\text{-}1}$ (***Figures 5B***), the
315 proximal *COOLAIR* isoform (type I.i) was still slightly detected by quantitative PCR (qPCR),
316 probably due to alternative TSSs (***Figure 5C***). However, the expression of the proximal *COOLAIR*
317 variant in the $FLC_{\Delta COOLAIR}$ mutant was not induced throughout the vernalization period, while the
318 wild type showed type I.i *COOLAIR* peaks at 1V and 20V (***Figure 5C***). Furthermore, *CBF3*
319 overexpression did not significantly increase type I.i *COOLAIR* levels in the $FLC_{\Delta COOLAIR\text{-}1}$ mutant,
320 while it caused a strong increase in proximal *COOLAIR* in the wild-type background (Col-0)
321 (***Figure 5—figure supplement 2***). Taken together, our results strongly suggest that the *COOLAIR*
322 promoter region containing the two CRT/DREs is necessary for the long-term cold response of
323 *COOLAIR*.

324

325 **CBFs-mediated *COOLAIR* induction during vernalization is not required for *FLC* silencing**

326 Finally, we investigated the role of *COOLAIR* induced by CBFs in the vernalization-triggered *FLC*
327 silencing process. *COOLAIR* was reported to facilitate the removal of H3K36me3 from *FLC*
328 chromatin during vernalization, whereas the other lncRNAs, *COLDAIR* and *COLDWRAP*, are
329 required for H3K27me3 deposition (*Csorba et al., 2014; Berry and Dean, 2015; Kim and Sung,*
330 *2017b; Zhu et al., 2021*). Therefore, we compared the enrichment of H3K4me3, H3K36me3, and

331 H3K27me3 on *FLC* chromatin in non-vernalized or vernalized wild-type and *cbfs* plants. As
332 reported (*Bastow et al., 2004; Sung and Amasino, 2004b; Yang et al., 2014*), the enrichments of
333 H3K4me3 and H3K36me3 were reduced, but that of H3K27me3 was increased in *FLC* chromatin
334 at 40V in the wild type (***Figures 6A to 6C***). However, although *COOLAIR* levels were significantly
335 reduced in the *cbfs* mutant (***Figure 4A***), vernalization-mediated reductions in H3K4me3 and
336 H3K36me3 levels and an increase in H3K27me3 levels in the *cbfs* mutant were comparable to
337 those in the wild type (***Figures 6A to 6C***). This result suggests that CBF-mediated *COOLAIR*
338 induction is not required for vernalization-induced epigenetic changes on *FLC* chromatin.

339 Consistent with the epigenetic changes, the *FLC* level in the *cbfs* mutant was gradually
340 suppressed during the vernalization process, and the suppression was maintained after 40VT4
341 similar to that observed in the wild type (***Figure 6D***). Such result is consistent with the RNA-seq
342 data previously reported using *cbfs* mutants in an SW ecotype (*S. Park et al., 2018*). RNA-seq data
343 analysis showed that the *cbfs* mutant in the SW background exhibited reduced *FLC* levels after
344 14V, similar to the wild type (***Figure 4—figure supplement 2***).

345 Because our results indicate that *COOLAIR* induction is not required for *FLC* silencing and
346 the function of *COOLAIR* in vernalization-induced *FLC* silencing is still debated (*Helliwell et al.,*
347 *2011; Csorba et al., 2014; Zhao et al., 2021; Zhu et al., 2021*), we analyzed whether the loss-of-
348 function mutations $FLC_{\Delta COOLAIR\text{-}1}$, and $FLC_{\Delta COOLAIR\text{-}3}$ result in any defect in the vernalization
349 response. In contrast to the transgenic lines used in previous reports, $FLC_{\Delta COOLAIR\text{-}1}$ and
350 $FLC_{\Delta COOLAIR\text{-}3}$, which have small deletions in the *COOLAIR* promoter region, are unlikely to cause
351 any unexpected effects on *FLC* chromatin. $FLC_{\Delta COOLAIR\text{-}4}$, which has a deletion outside of the
352 CRT/DRE region, exhibited a gradual decrease and eventual silencing of *FLC* by long-term cold,

353 similar to the wild type (***Figure 6E***). Interestingly, both $FLC_{\Delta COOLAIR\text{-}1}$ and $FLC_{\Delta COOLAIR\text{-}3}$ mutants
354 exhibited similar decreases and silencing of *FLC* by vernalization (***Figures 5B, 6D,* and *6E***).
355 These results show that *FLC* is normally silenced by vernalization regardless of *COOLAIR*
356 induction by cold.

357 Consistent with this, the *cbfs* mutant, compared to the wild type, did not show any difference
358 in the reduction of *FLC* levels upon exposure to a freezing cold for 8 h after NV, 10V, and 20V
359 (***Figure 6F***). However, the same freezing cold treatment caused the failure of strong induction of
360 *COOLAIR* in the *cbfs* (***Figure 4C***). These results also support that CBF-mediated *COOLAIR*
361 induction is not required for *FLC* silencing by vernalization.

362 As expected from the *FLC* levels, vernalization-mediated promotion of flowering was
363 comparable in the wild type and *cbfs* (***Figures 7A and 7B***), indicating that *cbfs* exhibits a normal
364 vernalization response. Consistently, the flowering time of $FLC_{\Delta COOLAIR\text{-}1}$ and $FLC_{\Delta COOLAIR\text{-}3}$ was
365 accelerated by vernalization, similar to that of the wild type (***Figures 7A, 7C, and 7D***). These
366 results show that *FLC* silencing occurs regardless of whether *COOLAIR* is induced during a cold
367 exposure that results in vernalization. In summary, our data strongly support that CBFs,
368 upregulated by long-term cold exposure, induce *COOLAIR* expression (***Figure 8***); however, cold-
369 mediated *COOLAIR* induction is not required for *FLC* silencing during vernalization.

370 ## Discussion

371

372 Winter is challenging for sessile plants: cold weather makes reproduction difficult, and frost
373 threatens survival. Cold acclimation and vernalization, the two types of low-temperature memories,
374 allow plants to overcome this harsh season by making them more viable during winter or flowering
375 in the subsequent warm spring (*Thomashow, 1999; Michaels and Amasino, 2000*). Although it is
376 well understood how plants recognize and remember short-term cold exposure to increase frost
377 hardiness, there is still much to know about the long-term cold sensing mechanism that establishes
378 the ability to flower.

379 *FLC* orthologs from a range of *A. thaliana* relatives express the vernalization-induced
380 antisense lncRNA, *COOLAIR* (*Castaings et al., 2014*). As the proximal sequence blocks within
381 the *COOLAIR* promoters are conserved, they are likely targets of cold sensor modules. This study
382 showed that CBF proteins act as cold sensors binding to the CRT/DREs in the conserved promoter
383 region, thereby activating the transcription of *COOLAIR*. Based on the data presented here, we
384 propose a working model (***Figure 8***) in which a prolonged low-temperature environment gradually
385 increases the levels of CBF proteins, which activate *COOLAIR* transcription in the early phase of
386 vernalization by binding to CRT/DREs at the 3′-end of *FLC*. However, as cold period extended,
387 CBF proteins are excluded from the *COOLAIR* promoter, probably because silencing of *FLC*
388 chromatin occurs regardless of CBFs level. This may account for a decrease in *COOLAIR* levels
389 during the later phase of vernalization. Consistent with this, a previous report showed a continuous
390 increase in the *COOLAIR* level throughout the vernalization period in the *vin3* mutant, which has
391 a defect in the maintenance of *FLC* silencing (*Swiezewski et al., 2009*). Thus, VIN3-dependent

392 Polycomb silencing is at least partially involved in the release of CBF proteins from the *COOLAIR*
393 promoter.

394 Although CBFs are upregulated by cold to trigger *COOLAIR* expression, CBF-mediated
395 *COOLAIR* induction during vernalization is not solely due to increased CBF levels because the
396 *CBF3* overexpression lines still showed *COOLAIR* induction by vernalization (***Figure 4B***). This
397 may indicate that additional factors participate in the regulation of CBFs function. As
398 aforementioned, it has previously been reported that low temperatures cause functional activation
399 of CBFs through the degradation of BTF3s and HD2C, which maintains an epigenetically inactive
400 state of downstream targets at warm temperatures (*Ding et al., 2018; J. Park et al., 2018*).
401 Moreover, cold triggers the monomerization of CBF proteins, thereby promoting their functions
402 (*Lee et al., 2021*). Similarly, such an additional regulatory mechanism of CBF function may be
403 enhanced by long-term winter cold to fine-tun *COOLAIR* expression.

404 In addition, other thermosensors are likely to facilitate *COOLAIR* induction by vernalization.
405 Recently, it was suggested that NTL8, an NAC domain-containing transcription factor, acts as an
406 upstream regulator of *COOLAIR* (*Zhao et al., 2021*). NTL8 also binds to the *COOLAIR* promoter
407 region, which is not far from CBF-binding sites (*O'Malley et al., 2016; Zhao et al., 2021*).
408 *COOLAIR* is highly expressed in both dominant mutant alleles, *ntl8-Ds*, and *NTL8*-overexpressing
409 transgenic plants at warm temperatures. Thus, it has been proposed that slow accumulation of the
410 NTL8 protein, due to reduced dilution during slower growth at low temperatures, causes
411 *COOLAIR* induction during vernalization. In addition, a WRKY transcription factor, WRKY63,
412 has been suggested as another inducer of *COOLAIR* transcription during vernalization (*Hung et*
413 *al., 2022*). WRKY63 is enriched in the *COOLAIR* promoter region, and *COOLAIR* expression is

414 reduced in the *wrky63* mutant, suggesting that WRKY63 functions as a *COOLAIR* activator.
415 Unlike NTL8, both transcript and protein levels of *WRKY63* were upregulated by vernalization,
416 which may lead to an increase in *COOLAIR* expression. Thus, it would be worthwhile to elucidate
417 whether NTL8, WRKY63, and CBFs synergistically activate *COOLAIR* transcription during
418 vernalization. The reason why vernalization-triggered *COOLAIR* induction requires more than one
419 thermosensor is unclear. Presumably, multiple thermosensory modules ensure precise and robust
420 *COOLAIR* expression during winter, when the temperature fluctuates.

421 Transcription of *COOLAIR* has been proposed to govern the *FLC* chromatin environment in
422 both warm and cold temperatures (*Csorba et al., 2014; Fang et al., 2020; Xu, Wu, et al., 2021*).
423 Previous studies have inferred that *COOLAIR* is required to remove H3K36me3 from *FLC*
424 chromatin, especially under low-temperature conditions. This argument is supported by the
425 delayed H3K36me3 removal in vernalized *FLC-TEX* transgenic plants, where the *COOLAIR*
426 promoter is substituted by the *rbcs3B* terminator sequence (*Csorba et al., 2014; Marquardt et al.,*
427 *2014; Wang et al., 2014*). In addition, *COOLAIR* is reported to promote condensation of FRI upon
428 cold exposure (*Zhu et al., 2021*). Thus, FRI is sequestered from the *FLC* promoter as a nuclear
429 condensate, which causes the transcriptional repression of *FLC*. Therefore, it has been suggested
430 that vernalization-induced *COOLAIR* prevents the activation of *FLC* by the FRI complex and
431 causes epigenetic silencing of *FLC* chromatin through a decrease of H3K36me3 during the
432 vernalization process.

433 However, there is some controversy as to whether *COOLAIR* is required for vernalization and
434 the associated *FLC* silencing. In contrast to the *FLC-TEX* lines, some T-DNA insertion lines which
435 lack *COOLAIR* induction by long-term cold exposure show a normal vernalization response

436 (*Helliwell et al., 2011*). Likewise, the results from this study show that *COOLAIR* transcription is
437 not required for the epigenetic silencing of *FLC*. The *cbfs* mutant, which exhibits severely reduced
438 *COOLAIR* induction, shows relatively normal vernalization responses such that flowering time is
439 fairly well accelerated and active histone marks, H3K36me3 and H3K4me3, are reduced in *FLC*
440 chromatin while the repressive histone mark, H3K27me3, is increased in *FLC* chromatin similar
441 to the wild type (***Figures 6 and 7***). Consistently, $FLC_{\Delta COOLAIR\text{-}1}$, and $FLC_{\Delta COOLAIR\text{-}3}$ mutants, which
442 have almost undetectable levels of *COOLAIR*, exhibit both *FLC* suppression and flowering
443 acceleration by vernalization similar to that seen in the wild type (***Figures 6 and 7***). Moreover, the
444 freezing treatment mimicking the first frost did not affect *FLC* suppression in the *cbfs*, although
445 the mutant showed defects in CBF-mediated *COOLAIR* induction (***Figures 4C and 6F***). It is
446 noteworthy that our finding that vernalization and the associated *FLC* silencing do not require
447 *COOLAIR* expression were obtained using *cbfs* and $FLC_{\Delta COOLAIR}$ mutant lines rather than the
448 transgenic lines used in previous studies. Thus, we can exclude the possibility that transgenes
449 somehow provide cryptic promoters or cause unexpected epigenetic effects.

450 *COOLAIR* is highly conserved among Arabidopsis relatives (*Castaings et al., 2014*); thus, our
451 finding that *COOLAIR* is not required for vernalization-induced *FLC* silencing is surprising. There
452 are several caveats in the studies of *COOLAIR* function. First, different experimental schemes may
453 affect the vernalization response differently. A recent study of plants grown in condition with
454 fluctuating temperatures designed to mimic natural environments may result in a role for
455 *COOLAIR* in vernalization-mediated *FLC* repression (*Zhao et al., 2021*), and perhaps fluctuating
456 temperatures that mimic field conditions may have different effects on the vernalization response
457 of *cbfs* or $FLC_{\Delta COOLAIR}$ mutants as well. However, the experiments in most studies that claimed a

role for *COOLAIR* in vernalization were performed in laboratory conditions with controlled temperatures as in this study. If indeed *COOLAIR* does have a role in vernalization in specific environmental conditions, the lack of a role for *COOLAIR* in vernalization in other conditions such as those in this study may be due to functional redundancy between *COOLAIR* and other *FLC* repressors such that other repressors, such as *COLDAIR*, obscure the effect of *COOLAIR* on *FLC* silencing, as has been proposed before (*Castaings et al., 2014*). This issue should be addressed in future studies.

Although short-term and long-term cold memories elicit different developmental responses, both are triggered by the same physical environment. Therefore, it is not surprising that a common signaling network governs both processes. *CBF* genes have been highlighted for their roles in cold acclimation (*Gilmour et al., 1998; Liu et al., 1998; Jia et al., 2016; Zhao et al., 2016*). CBFs rapidly accumulate upon short-term cold exposure, thereby activating the transcription of cold-responsive genes, such as *COR15A* and *RD29A* (*Stockinger et al., 1997; Liu et al., 1998*). Interestingly, CBFs are also highly accumulated during vernalization and mediate long-term cold-induced *COOLAIR* expression. Hence, our results indicate that the cold signaling pathways that establish the short-term and long-term cold responses are not sharply distinguishable, as suggested previously (*Sung and Amasino, 2004a; Seo et al., 2009*).

475 # Materials and Methods

476

477 **Plant materials and treatments**

478 *Arabidopsis thaliana* Columbia-0 (Col-0), Wassilewskija-2 (Ws-2), and Col:*FRI*^{Sf2} (*FRI* Col) were
479 used as the wild types in this study. "Wild type" in this paper mainly refers to *FRI* Col unless
480 otherwise specified. The *FRI* Col (*Lee et al., 1994*), *cbfs-1*, *pCBF3:CBF3-myc* (*Jia et al., 2016*),
481 *pSuper:CBF3-myc* (*Liu et al., 2017*), *FLC*$_{\Delta COOLAIR-1}$ (*Luo et al., 2019*), *35S:CBF1*, *35S:CBF2*, and
482 *35S:CBF3* (*Gilmour et al., 2004*) have been previously described. *FRI cbfs-1* was generated by
483 crossing the *FRI* Col with *cbfs-1* stated above. *FRI FLC*$_{\Delta COOLAIR-1}$ was generated by crossing *FRI*
484 Col with *FLC*$_{\Delta COOLAIR-1}$ in the Col-0 background, as described above. *pSuper:CBF3-myc*
485 *FLC*$_{\Delta COOLAIR-1}$ was generated by crossing *pSuper:CBF3-myc* with *FLC*$_{\Delta COOLAIR-1}$. For all
486 experiments using plant materials, seeds were sown on half-strength Murashige & Skoog (MS)
487 medium (Duchefa, Haarlem, Netherlands) containing 1% sucrose and 1% plant agar (Duchefa)
488 and stratified at 4°C for 3 days. Plants were germinated and grown at 22°C under a short-day (SD)
489 cycle (8 h light/16 h dark) with cool white fluorescent lights (100 μmol m^{-2} s^{-1}). For the
490 vernalization treatment, the plants were grown at 22°C for the prescribed period and then
491 transferred to a 4°C growth chamber under an SD cycle. To adjust the developmental stage, the
492 plants vernalized for 40 days (40V), 30 days (30V), 20 days (20V), 10 days (10V), 4 days (4V),
493 and 1 day (1V) were transferred to 4°C after being grown at 22°C for 10, 12, 14, 15, and 16 days,
494 respectively. Non-vernalized (NV) plants were grown at 22°C for 16 days. For 0. 0.5, 1, 1.5, 2, 3,
495 6, and 24 h of cold treatment, the plants were grown at 22°C for 16 days before the 4°C treatment.
496 For the freezing treatment, NV, 10V, and 20V plants were transferred to −1°C under dark condition

497 for 8 h (F). To measure flowering time of vernalized plants, plants were transferred to 22°C under
498 a long-day (LD) cycle (16 h light/8 h dark) directly after the vernalization treatment.
499
500 **Generation of *FLC$_{\Delta COOLAIR}$* lines by CRISPR-Cas9**
501 The construction of *FLC$_{\Delta COOLAIR\text{-}3}$* and *FLC$_{\Delta COOLAIR\text{-}4}$* are as previously described (*Luo et al., 2019*).
502 Briefly, two pairs of sgRNAs were designed for the deletion of *COOLAIR* promoter regions (5′-
503 CTTCACAGTGAAGAAGCCTA-3′ and 5′-AAATGCACTCTTACGTAACG-3′ for *FLC$_{\Delta COOLAIR\text{-}3}$*;
504 5′-TTATCCTAAACGCGTATGGT-3′ and 5′-CGTAGTTCCGTCATCCATGA-3′ for
505 *FLC$_{\Delta COOLAIR\text{-}4}$*), and sgRNA-Cas9 cassettes were introduced into Arabidopsis by floral dipping.
506 Homozygous deletion mutants were screened in T_2 generation, and *sgRNA-Cas9* free mutants were
507 further isolated in T_3 generation.
508
509 **Plasmid construction**
510 To generate the *35S:CBF3-HA* construct, the entire coding sequence of CBF3 was amplified using
511 PCR and cloned into the *HBT-HA-NOS* plasmid (*Yoo et al., 2007*). For *pCOOLAIR$_{DRE}$:LUC* and
512 *pCOOLAIR$_{DRE}^{m}$:LUC* construction, the 1-kb sequence containing the *COOLAIR* promoter, the 3′-
513 untranslated region (UTR), and the last exon of *FLC* was amplified by PCR and cloned into the
514 *LUC-NOS* plasmid (*Hwang and Sheen, 2001*). To generate *pCOOLAIR$_{DRE}^{m}$:LUC*, two CRT/DREs
515 in the *COOLAIR* promoter, 5′-AGGTCGGT-3′ and 5′-ACCGACAT-3′, were replaced with 5′-
516 CGAGGTGT-3′ and 5′-TGAACCCA-3′, respectively. For *pFLC:LUC* construction, the 1-kb
517 sequence containing the promoter, 5′-UTR, and the first exon of *FLC* was amplified by PCR and
518 was cloned into the *LUC-NOS* plasmid.

519

520 **Electrophoretic mobility shift assay (EMSA)**

521 Maltose binding protein (MBP) and MBP-CBF3 recombinant fusion proteins were induced by 500
522 μM isopropyl β-D-thiogalactoside (IPTG) in the *E. coli* BL21 (DE3) strain. Cell extracts were
523 isolated with a buffer containing 20 mM Tris-HCl (pH 7.4), 1 mM EDTA, 200 mM NaCl, 10%
524 glycerol, 1 mM DTT, and 1 mM PMSF. Proteins were purified from cell extracts using MBPTrap™
525 HP column (GE Healthcare, Chicago, IL, USA) with ÄKTA FPLC system (Amersham Biosciences,
526 Amersham, UK). The Cy5-labeled probes and unlabeled competitors were generated by annealing
527 25 bp-length oligonucleotides. EMSA was performed as previously described with a few
528 modifications (*Seo et al., 2012*). For each EMSA reaction, 5 μM of protein and 100 nM of Cy5-
529 labeled probe were incubated at room temperature in a binding buffer containing 10 mM Tris-HCl
530 (pH 7.5), 1 mM EDTA, 50 mM NaCl, 5% glycerol, and 5 mM DTT. For the competition assay, the
531 reaction mixtures were incubated in the presence of 100-fold molar excess of each competitor. The
532 reaction mixtures were electrophoresed at 100 V after incubation. The Cy5 signals were detected
533 using WSE-6200H LuminoGraph II (ATTO, Amherst, NY, USA).

534

535 **Chromatin immunoprecipitation (ChIP) assay**

536 Approximately 4 g of seedlings grown on MS plates was collected and cross-linked using 1% (v/v)
537 formaldehyde. Nuclei were isolated from seedlings using a buffer containing 20 mM PIPES-KOH
538 (pH 7.6), 1 M hexylene glycol, 10 mM $MgCl_2$, 0.1 mM EGTA, 15 mM NaCl, 60 mM KCl, 0.5%
539 Triton-X, 5 mM β-mercaptoethanol, and 1× cOmplete™ EDTA-free Protease Inhibitor Cocktail
540 (Roche, Basel, Switzerland) as described previously with a few modifications (*Shu et al., 2014*).

541 Isolated nuclei were lysed with a buffer containing 50 mM Tris-HCl (pH 7.4), 150 mM NaCl, 1%
542 (v/v) Triton X-100, and 1% SDS (w/v), and were subsequently sonicated using a Digital Sonifier®
543 (Branson, Danbury, CT, USA). Sheared chromatin was diluted with a buffer containing 50 mM
544 Tris-HCl (pH 7.4), 150 mM NaCl, 1% (v/v) Triton X-100, and 1 mM EDTA. Immunoprecipitation
545 was performed by incubating sheared chromatin with Protein G Sepharose™ 4 Fast Flow beads
546 (GE Healthcare) and antibodies. Anti-myc (MBL, Woburn, MA, USA, #M192-3) and normal
547 mouse IgG_1 (Santa Cruz Biotechnology, Santa Cruz, CA, USA, #sc-3877) were used to detect
548 CBF3 protein enrichment at the *FLC* locus, and anti-H3K36me3 (Abcam, Cambridge, UK,
549 #Ab9050), H3K4me3 (Millipore, Bedford, MA, USA, #07-473), and anti-H3K27me3 (Millipore,
550 #07-449) were used to detect histone modifications on the *FLC* chromatin. DNA was extracted
551 with phenol:chloroform:isoamyl alcohol (25:24:1, v/v) or Chelex® 100 Resin according to the
552 manufacturer's instruction.
553
554 **Gene expression analysis**
555 Total RNA was isolated from ~100 mg of seedlings grown on MS agar plate using TRI Reagent®
556 (Sigma-Aldrich, St Louis, MO, USA) or TS™ Plant Mini Kit (Taeshin Bio Science, Gyeonggi-do,
557 Korea). cDNA was generated using 4 μg of total RNA, 5 units of recombinant DNase I (TaKaRa,
558 Kyoto, Japan), 200 units of RevertAid™ reverse transcriptase (Thermo Scientific, Waltham, MA,
559 USA), and buffer containing 0.25 mM dNTP and 0.1 μg oligo$(dT)_{18}$. Quantitative PCR analysis
560 was performed using iQ™ SYBR® Green Supermix (Bio-Rad, Hercules, CA, USA) and a CFX96
561 Real-Time PCR system (Bio-Rad).
562 To examine *COOLAIR* expression in the *COOLAIR* promoter deletions lines, Total RNAs

563 were extracted using the RNeasy® Plus Mini Kit (Qiagen, Hilden, Germany) according to the
564 manufacturers' instructions, followed by the digestion of residual genomic DNA by the gDNA
565 wiper (Vazyme, Nanjing, China). 1.0-μg RNA from each sample was taken for cDNA synthesis
566 using the HiScript® III 1st Strand cDNA Synthesis Kit (Vazyme) with the transcript-specific
567 primers (5′-TGGTTGTTATTTGGTGGTGTGAA-3′ for *COOLAIR* class I and 5′-
568 GCCCGACGAAGAAAAAGTAG-3′ for class II). Semi-quantitative PCR amplifications was
569 performed, followed by agarose gel separation of PCR products.
570

571 **Immunoblotting**

572 Total protein was isolated from ~100 mg of seedlings using a buffer containing 50 mM Tris-HCl
573 (pH 7.5), 100 mM NaCl, 10 mM $MgCl_2$, 1 mM EDTA, 10% glycerol, 1 mM PMSF, 1 mM DTT
574 and 1× cOmplete™ EDTA-free Protease Inhibitor Cocktail (Roche). Fifty micrograms of total
575 protein were loaded onto SDS-PAGE gels and separated by electrophoresis. The proteins were
576 transferred to PVDF membranes (Amersham Biosciences) and probed with an anti-myc (MBL,
577 #M192-3; 1:10000 dilution) antibody overnight at 4°C. The samples were then probed with
578 horseradish peroxidase (HRP)-conjugated anti-mouse IgG (Cell Signaling, Danvers, MA, USA,
579 #7076; 1:10000 dilution) antibody at room temperature. The signals were detected with
580 ImageQuant™ LAS 4000 (GE Healthcare) using WesternBright™ Sirius ECL solution (Advansta,
581 San Jose, CA, USA).
582

583 **RNA sequencing (RNA-seq) data analysis**

584 We retrieved two sets of RNA-seq data from the NCBI SRA-numbered SRP056607 and

585 SRP320943. SRP056607 contains raw reads from NV, 1V, and 14V wild-type and *cbfs* plants in a
586 Sweden-ecotype (SW) background. SRP3209943 contains reads from 0, 3, and 24 h cold-treated
587 wild-type and *cbfs* plants in a Col-0 background. The reads were aligned to the Arabidopsis TAIR
588 10 reference genome and annotated in ARAPORT 11 using STAR version 2.7.10a. Isoform
589 estimation was performed using Salmon version 1.6.0.
590

591 **Luciferase assay using Arabidopsis protoplast**

592 Protoplast isolation and transfection were performed as previously described with some
593 modifications (*Yoo et al., 2007*). Protoplasts were isolated from leaves of SD-grown wild-type
594 plant (Col-0) using a buffer containing 150 mg Cellulase Onozuka™ R-10 (Yakult, Tokyo, Japan),
595 50 mg Maceroenzyme™ R-10 (Yakult), 20 mM KCl, 20 mM MES-KOH (pH 5.6), 0.4 M D-
596 mannitol, 10 mM $CaCl_2$, 5 mM β-mercaptoethanol, and 0.1 g bovine serum albumin. For protoplast
597 transfection, 200 μg of plasmid DNA and isolated protoplasts were incubated in a buffer containing
598 0.1 M D-mannitol, 50 mM $CaCl_2$, and 20% (w/v) PEG. Luciferase activity in the protoplasts was
599 measured using the Luciferase Assay System (Promega, Madison, WI, USA) and MicroLumat
600 Plus LB96V microplate luminometer (Berthold Technologies, Bad Wildbad, Germany).

601 ## Supplementary data

602 **Figure 1—figure supplement 1.** CBF proteins directly bind to the sequence at the 3′-end of *FLC*
603 in DNA affinity purification sequencing (DAP-seq).

604 **Figure 1—figure supplement 2.** CBF3 binds to DRE1 and DRE2 on the *COOLAIR* promoter and
605 DREc on the first exon of *FLC.*

606 **Figure 2—figure supplement 1.** Overexpression of *CBF1*, *2*, or *3* causes an increase in *COOLAIR*
607 level, but the effects on *COOLAIR* variants are subtly different.

608 **Figure 3—figure supplement 1.** Vernalization increases CBF3 protein levels with a minor effect
609 on the daily rhythm.

610 **Figure 4—figure supplement 1.** CBF regulons show strongly reduced expression in *cbfs* mutants
611 similar to *COOLAIR*.

612 **Figure 4—figure supplement 2.** Cold-triggered *COOLAIR* expression is impaired in *cbfs* mutants
613 in Col-0 and Sweden-ecotype background.

614 **Figure 4—figure supplement 3.** Freezing temperature increases the levels of *CBFs*.

615 **Figure 5—figure supplement 1.** Genomic sequences near the deleted regions in two *COOLAIR*
616 promoter deletion lines, $FLC_{\Delta COOLAIR\text{-}3}$ and $FLC_{\Delta COOLAIR\text{-}4}$.

617 **Figure 5—figure supplement 2.** Proximal *COOLAIR* level is not significantly increased by *CBF3*
618 overexpression in the $FLC_{\Delta COOLAIR}$ mutant lacking CRT/DREs.

619 **Figure 1—source data 1.** Uncropped labelled gel image and the original image file for the EMSA
620 result.

621 **Figure 1—figure supplement 2—source data 1.** Uncropped labelled gel images and the original
622 image files for the EMSA results.

Figure 3—source data 1. Uncropped labelled blot images and the original image files for the immunoblots.

Figure 3—figure supplement 1—source data 1. Uncropped labelled blot images and the original image files for the immunoblots.

Figure 5—source data 1. Uncropped labelled gel images and the original image files for the RT-PCR results.

Supplementary File 1. Oligonucleotide sequences used in this study.

Acknowledgements

We would like to thank Dr. Shuhua Yang (China Agricultural University, China) for providing the *cbfs-1*, *pCBF3:CBF3-myc*, and *pSuper:CBF3-myc* seeds. This work was supported by the Cooperative Research Program for Agriculture Science and Technology Development (No. PJ01315201 and PJ01315401), Rural Development Administration, Republic of Korea. This work was also supported by National Research Foundation of Korea (NRF) grants funded by the Korean government (MSIT) (No. 2019R1A2C2004313 and NRF-2021R1A5A1032428). Y. He's laboratory was funded by the grants from the National Natural Science Foundation of China (No. 31830049 and 31721001). M. Jeon and D. Jeong were supported by Brain Korea 21 Plus Project. We would like to thank Editage (http://www.editage.co.kr) for English language editing.

643 ## References

644

645 Angel A, Song J, Dean C, Howard M (2011) **A Polycomb-based switch underlying quantitative**
646 **epigenetic memory**. *Nature* **476:** 105-108. https://doi.org/10.1038/nature10241

647 Baker SS, Wilhelm KS, Thomashow MF (1994) **The 5'-region of *Arabidopsis thaliana cor15a***
648 **has *cis*-acting elements that confer cold-, drought- and ABA-regulated gene**
649 **expression**. *Plant Mol Biol* **24:** 701-713. https://doi.org/10.1007/BF00029852

650 Bastow R, Mylne JS, Lister C, Lippman Z, Martienssen RA, Dean C (2004) **Vernalization**
651 **requires epigenetic silencing of *FLC* by histone methylation**. *Nature* **427:** 164-167.
652 https://doi.org/10.1038/nature02269

653 Berry S, Dean C (2015) **Environmental perception and epigenetic memory: Mechanistic**
654 **insight through *FLC***. *Plant J* **83:** 133-148. https://doi.org/10.1111/tpj.12869

655 Castaings L, Bergonzi S, Albani MC, Kemi U, Savolainen O, Coupland G (2014) **Evolutionary**
656 **conservation of cold-induced antisense RNAs of *FLOWERING LOCUS C* in**
657 ***Arabidopsis thaliana* perennial relatives**. *Nat Commun* **5:** 4457.
658 https://doi.org/10.1038/ncomms5457

659 Chinnusamy V, Zhu J, Zhu JK (2007) **Cold stress regulation of gene expression in plants**. *Trends*
660 *Plant Sci* **12:** 444-451. https://doi.org/10.1016/j.tplants.2007.07.002

661 Choi K, Kim J, Hwang HJ, Kim S, Park C, Kim SY, Lee I (2011) **The FRIGIDA complex**
662 **activates transcription of *FLC*, a strong flowering repressor in *Arabidopsis*, by**
663 **recruiting chromatin modification factors**. *Plant Cell* **23:** 289-303.
664 https://doi.org/10.1105/tpc.110.075911

665 Chouard P (1960) **Vernalization and its relations to dormancy**. *Annu Rev Plant Phys* **11:** 191-
666 238. https://doi.org/10.1146/annurev.pp.11.060160.001203

667 Csorba T, Questa JI, Sun Q, Dean C (2014) **Antisense *COOLAIR* mediates the coordinated**
668 **switching of chromatin states at *FLC* during vernalization**. *Proc Natl Acad Sci U S A*
669 **111:** 16160-16165. https://doi.org/10.1073/pnas.1419030111

670 De Lucia F, Crevillen P, Jones AM, Greb T, Dean C (2008) **A PHD-Polycomb Repressive**
671 **Complex 2 triggers the epigenetic silencing of *FLC* during vernalization**. *Proc Natl*

672 *Acad Sci U S A* **105:** 16831-16836. https://doi.org/10.1073/pnas.0808687105
673 Ding Y, Jia Y, Shi Y, Zhang X, Song C, Gong Z, Yang S (2018) **OST1-mediated BTF3L**
674 **phosphorylation positively regulates CBFs during plant cold responses**. *EMBO J* **37**.
675 https://doi.org/10.15252/embj.201798228
676 Ding Y, Shi Y, Yang S (2019) **Advances and challenges in uncovering cold tolerance regulatory**
677 **mechanisms in plants**. *New Phytol* **222:** 1690-1704. https://doi.org/10.1111/nph.15696
678 Ding Y, Yang S (2022) **Surviving and thriving: How plants perceive and respond to**
679 **temperature stress**. *Dev Cell* **57:** 947-958. https://doi.org/10.1016/j.devcel.2022.03.010
680 Doherty CJ, Van Buskirk HA, Myers SJ, Thomashow MF (2009) **Roles for *Arabidopsis* CAMTA**
681 **transcription factors in cold-regulated gene expression and freezing tolerance**. *Plant*
682 *Cell* **21:** 972-984. https://doi.org/10.1105/tpc.108.063958
683 Dong MA, Farré EM, Thomashow MF (2011) **CIRCADIAN CLOCK-ASSOCIATED 1 and**
684 **LATE ELONGATED HYPOCOTYL regulate expression of the C-REPEAT**
685 **BINDING FACTOR (CBF) pathway in *Arabidopsis***. *Proc Natl Acad Sci U S A* **108:**
686 7241-7246. https://doi.org/10.1073/pnas.1103741108
687 Eremina M, Unterholzner SJ, Rathnayake AI, Castellanos M, Khan M, Kugler KG, May ST, Mayer
688 KF, Rozhon W, Poppenberger B (2016) **Brassinosteroids participate in the control of**
689 **basal and acquired freezing tolerance of plants**. *Proc Natl Acad Sci U S A* **113:** E5982-
690 E5991. https://doi.org/10.1073/pnas.1611477113
691 Fang X, Wang L, Ishikawa R, Li Y, Fiedler M, Liu F, Calder G, Rowan B, Weigel D, Li P, Dean C
692 (2019) ***Arabidopsis* FLL2 promotes liquid-liquid phase separation of polyadenylation**
693 **complexes**. *Nature* **569:** 265-269. https://doi.org/10.1038/s41586-019-1165-8
694 Fang X, Wu Z, Raitskin O, Webb K, Voigt P, Lu T, Howard M, Dean C (2020) **The 3' processing**
695 **of antisense RNAs physically links to chromatin-based transcriptional control**. *Proc*
696 *Natl Acad Sci U S A* **117:** 15316-15321. https://doi.org/10.1073/pnas.2007268117
697 Finnegan EJ, Bond DM, Buzas DM, Goodrich J, Helliwell CA, Tamada Y, Yun JY, Amasino RM,
698 Dennis ES (2011) **Polycomb proteins regulate the quantitative induction of**
699 ***VERNALIZATION INSENSITIVE 3* in response to low temperatures**. *Plant J* **65:** 382-
700 391. https://doi.org/10.1111/j.1365-313X.2010.04428.x

701 Fowler S, Thomashow MF (2002) **Arabidopsis transcriptome profiling indicates that multiple**
702 **regulatory pathways are activated during cold acclimation in addition to the CBF cold**
703 **response pathway**. *Plant Cell* **14:** 1675-1690. https://doi.org/10.1105/tpc.003483
704 Gilmour SJ, Fowler SG, Thomashow MF (2004) **Arabidopsis transcriptional activators CBF1,**
705 **CBF2, and CBF3 have matching functional activities**. *Plant Mol Biol* **54:** 767-781.
706 https://doi.org/10.1023/B:PLAN.0000040902.06881.d4
707 Gilmour SJ, Hajela RK, Thomashow MF (1988) **Cold acclimation in *Arabidopsis thaliana***. *Plant*
708 *Physiol* **87:** 745-750. https://doi.org/10.1104/pp.87.3.745
709 Gilmour SJ, Zarka DG, Stockinger EJ, Salazar MP, Houghton JM, Thomashow MF (1998) **Low**
710 **temperature regulation of the *Arabidopsis* CBF family of AP2 transcriptional**
711 **activators as an early step in cold-induced *COR* gene expression**. *Plant J* **16:** 433-442.
712 https://doi.org/10.1046/j.1365-313x.1998.00310.x
713 Guy CL (1990) **Cold acclimation and freezing stress tolerance: Role of protein metabolism**.
714 *Annu Rev Plant Physiol Plant Mol Biol* **41:** 187-223.
715 https://doi.org/10.1146/annurev.pp.41.060190.001155
716 Hajela RK, Horvath DP, Gilmour SJ, Thomashow MF (1990) **Molecular cloning and expression**
717 **of *cor* (*co*ld-*r*egulated) genes in *Arabidopsis thaliana***. *Plant Physiol* **93:** 1246-1252.
718 https://doi.org/10.1104/pp.93.3.1246
719 Helliwell CA, Robertson M, Finnegan EJ, Buzas DM, Dennis ES (2011) **Vernalization-**
720 **repression of Arabidopsis *FLC* requires promoter sequences but not antisense**
721 **transcripts**. *PLoS One* **6:** e21513. https://doi.org/10.1371/journal.pone.0021513
722 Helliwell CA, Wood CC, Robertson M, James Peacock W, Dennis ES (2006) **The Arabidopsis**
723 **FLC protein interacts directly *in vivo* with *SOC1* and *FT* chromatin and is part of a**
724 **high-molecular-weight protein complex**. *Plant J* **46:** 183-192.
725 https://doi.org/10.1111/j.1365-313X.2006.02686.x
726 Heo JB, Sung S (2011) **Vernalization-mediated epigenetic silencing by a long intronic**
727 **noncoding RNA**. *Science* **331:** 76-79. https://doi.org/10.1126/science.1197349
728 Hung FY, Shih YH, Lin PY, Feng YR, Li C, Wu K (2022) **WRKY63 transcriptional activation**
729 **of *COOLAIR* and *COLDAIR* regulates vernalization-induced flowering**. *Plant Physiol*.

730 https://doi.org/10.1093/plphys/kiac295
731 Hwang I, Sheen J (2001) **Two-component circuitry in *Arabidopsis* cytokinin signal**
732 **transduction**. *Nature* **413:** 383-389. https://doi.org/10.1038/35096500
733 Jia Y, Ding Y, Shi Y, Zhang X, Gong Z, Yang S (2016) **The *cbfs* triple mutants reveal the essential**
734 **functions of *CBFs* in cold acclimation and allow the definition of CBF regulons in**
735 ***Arabidopsis***. *New Phytol* **212:** 345-353. https://doi.org/10.1111/nph.14088
736 Johanson U, West J, Lister C, Michaels S, Amasino R, Dean C (2000) **Molecular analysis of**
737 ***FRIGIDA*, a major determinant of natural variation in *Arabidopsis* flowering time**.
738 *Science* **290:** 344-347. https://doi.org/10.1126/science.290.5490.344
739 Kidokoro S, Yoneda K, Takasaki H, Takahashi F, Shinozaki K, Yamaguchi-Shinozaki K (2017)
740 **Different cold-signaling pathways function in the responses to rapid and gradual**
741 **decreases in temperature**. *Plant Cell* **29:** 760-774. https://doi.org/10.1105/tpc.16.00669
742 Kim DH, Sung S (2013) **Coordination of the vernalization response through a *VIN3* and *FLC***
743 **gene family regulatory network in *Arabidopsis***. *Plant Cell* **25:** 454-469.
744 https://doi.org/10.1105/tpc.112.104760
745 Kim DH, Sung S (2017a) **The binding specificity of the PHD-finger domain of VIN3 moderates**
746 **vernalization response**. *Plant Physiol* **173:** 1258-1268.
747 https://doi.org/10.1104/pp.16.01320
748 Kim DH, Sung S (2017b) **Vernalization-triggered intragenic chromatin loop formation by**
749 **long noncoding RNAs**. *Dev Cell* **40:** 302-312 e304.
750 https://doi.org/10.1016/j.devcel.2016.12.021
751 Kim DH, Zografos BR, Sung S (2010) **Mechanisms underlying vernalization-mediated *VIN3***
752 **induction in Arabidopsis**. *Plant Signal Behav* **5:** 1457-1459.
753 https://doi.org/10.4161/psb.5.11.13465
754 Kim Y, Park S, Gilmour SJ, Thomashow MF (2013) **Roles of CAMTA transcription factors and**
755 **salicylic acid in configuring the low-temperature transcriptome and freezing**
756 **tolerance of Arabidopsis**. *Plant J* **75:** 364-376. https://doi.org/10.1111/tpj.12205
757 Kyung J, Jeon M, Jeong G, Shin Y, Seo E, Yu J, Kim H, Park CM, Hwang D, Lee I (2022) **The**
758 **two clock proteins CCA1 and LHY activate *VIN3* transcription during vernalization**

759 **through the vernalization-responsive cis-element**. *Plant Cell* **34:** 1020-1037.
760 https://doi.org/10.1093/plcell/koab304
761 Lee ES, Park JH, Wi SD, Kang CH, Chi YH, Chae HB, Paeng SK, Ji MG, Kim WY, Kim MG,
762 Yun DJ, Stacey G, Lee SY (2021) **Redox-dependent structural switch and CBF**
763 **activation confer freezing tolerance in plants**. *Nat Plants* **7:** 914-922.
764 https://doi.org/10.1038/s41477-021-00944-8
765 Lee H, Suh SS, Park E, Cho E, Ahn JH, Kim SG, Lee JS, Kwon YM, Lee I (2000) **The**
766 **AGAMOUS-LIKE 20 MADS domain protein integrates floral inductive pathways in**
767 ***Arabidopsis***. *Genes Dev* **14:** 2366-2376. https://doi.org/10.1101/gad.813600
768 Lee I, Bleecker A, Amasino R (1993) **Analysis of naturally occurring late flowering in**
769 ***Arabidopsis thaliana***. *Mol Gen Genet* **237:** 171-176. https://doi.org/10.1007/BF00282798
770 Lee I, Michaels SD, Masshardt AS, Amasino RM (1994) **The late-flowering phenotype of**
771 ***FRIGIDA* and mutations in *LUMINIDEPENDENS* is suppressed in the Landsberg**
772 ***erecta* strain of *Arabidopsis***. *Plant J* **6:** 903-909. https://doi.org/10.1046/j.1365-
773 313X.1994.6060903.x
774 Li H, Ye K, Shi Y, Cheng J, Zhang X, Yang S (2017) **BZR1 positively regulates freezing**
775 **tolerance via CBF-dependent and CBF-independent pathways in *Arabidopsis***. *Mol*
776 *Plant* **10:** 545-559. https://doi.org/10.1016/j.molp.2017.01.004
777 Li Z, Jiang D, He Y (2018) **FRIGIDA establishes a local chromosomal environment for**
778 ***FLOWERING LOCUS C* mRNA production**. *Nat Plants* **4:** 836-846.
779 https://doi.org/10.1038/s41477-018-0250-6
780 Liu F, Marquardt S, Lister C, Swiezewski S, Dean C (2010) **Targeted 3' processing of antisense**
781 **transcripts triggers *Arabidopsis FLC* chromatin silencing**. *Science* **327:** 94-97.
782 https://doi.org/10.1126/science.1180278
783 Liu F, Quesada V, Crevillén P, Bäurle I, Swiezewski S, Dean C (2007) **The *Arabidopsis* RNA-**
784 **binding protein FCA requires a lysine-specific demethylase 1 homolog to**
785 **downregulate *FLC***. *Mol Cell* **28:** 398-407. https://doi.org/10.1016/j.molcel.2007.10.018
786 Liu Q, Kasuga M, Sakuma Y, Abe H, Miura S, Yamaguchi-Shinozaki K, Shinozaki K (1998) **Two**
787 **transcription factors, DREB1 and DREB2, with an EREBP/AP2 DNA binding**

788 **domain separate two cellular signal transduction pathways in drought- and low-**
789 **temperature-responsive gene expression, respectively, in Arabidopsis**. *Plant Cell* **10:**
790 1391-1406. https://doi.org/10.1105/tpc.10.8.1391
791 Liu Z, Jia Y, Ding Y, Shi Y, Li Z, Guo Y, Gong Z, Yang S (2017) **Plasma membrane CRPK1-**
792 **mediated phosphorylation of 14-3-3 proteins induces their nuclear import to fine-tune**
793 **CBF signaling during cold response**. *Mol Cell* **66:** 117-128 e115.
794 https://doi.org/10.1016/j.molcel.2017.02.016
795 Luo X, Chen T, Zeng X, He D, He Y (2019) **Feedback regulation of *FLC* by *FLOWERING***
796 ***LOCUS T* (*FT*) and *FD* through a 5' *FLC* promoter region in *Arabidopsis***. *Mol Plant*
797 **12:** 285-288. https://doi.org/10.1016/j.molp.2019.01.013
798 Marquardt S, Raitskin O, Wu Z, Liu F, Sun Q, Dean C (2014) **Functional consequences of**
799 **splicing of the antisense transcript *COOLAIR* on *FLC* transcription**. *Mol Cell* **54:** 156-
800 165. https://doi.org/10.1016/j.molcel.2014.03.026
801 Maruyama K, Sakuma Y, Kasuga M, Ito Y, Seki M, Goda H, Shimada Y, Yoshida S, Shinozaki K,
802 Yamaguchi-Shinozaki K (2004) **Identification of cold-inducible downstream genes of**
803 **the *Arabidopsis* DREB1A/CBF3 transcriptional factor using two microarray systems**.
804 *Plant J* **38:** 982-993. https://doi.org/10.1111/j.1365-313X.2004.02100.x
805 McKhann HI, Gery C, Bérard A, Lévêque S, Zuther E, Hincha DK, De Mita S, Brunel D, Téoulé
806 E (2008) **Natural variation in CBF gene sequence, gene expression and freezing**
807 **tolerance in the Versailles core collection of Arabidopsis thaliana**. *BMC Plant Biol* **8:**
808 105. https://doi.org/10.1186/1471-2229-8-105
809 Medina J, Bargues M, Terol J, Pérez-Alonso M, Salinas J (1999) **The Arabidopsis *CBF* gene**
810 **family is composed of three genes encoding AP2 domain-containing proteins whose**
811 **expression Is regulated by low temperature but not by abscisic acid or dehydration**.
812 *Plant Physiol* **119:** 463-470. https://doi.org/10.1104/pp.119.2.463
813 Michaels SD, Amasino RM (1999) ***FLOWERING LOCUS C* encodes a novel MADS domain**
814 **protein that acts as a repressor of flowering**. *Plant Cell* **11:** 949-956.
815 https://doi.org/10.1105/tpc.11.5.949
816 Michaels SD, Amasino RM (2000) **Memories of winter: Vernalization and the competence to**

817 **flower**. *Plant Cell Environ* **23:** 1145-1153. https://doi.org/10.1046/j.1365-
818 3040.2000.00643.x
819 Michaels SD, Amasino RM (2001) **Loss of *FLOWERING LOCUS C* activity eliminates the late-**
820 **flowering phenotype of *FRIGIDA* and autonomous pathway mutations but not**
821 **responsiveness to vernalization**. *Plant Cell* **13:** 935-941.
822 https://doi.org/10.1105/tpc.13.4.935
823 Michaels SD, Himelblau E, Kim SY, Schomburg FM, Amasino RM (2005) **Integration of**
824 **flowering signals in winter-annual Arabidopsis**. *Plant Physiol* **137:** 149-156.
825 https://doi.org/10.1104/pp.104.052811
826 Mylne JS, Barrett L, Tessadori F, Mesnage S, Johnson L, Bernatavichute YV, Jacobsen SE, Fransz
827 P, Dean C (2006) **LHP1, the *Arabidopsis* homologue of HETEROCHROMATIN**
828 **PROTEIN1, is required for epigenetic silencing of *FLC***. *Proc Natl Acad Sci U S A* **103:**
829 5012-5017. https://doi.org/10.1073/pnas.0507427103
830 Napp-Zinn K (1955) **Genetische grundlagen des Kältebedürfnisses bei *Arabidopsis thaliana***
831 **(L.) Heynh**. *Naturwissenschaften* **42:** 650-650. https://doi.org/10.1007/Bf00622395
832 Nishio H, Buzas DM, Nagano AJ, Suzuki Y, Sugano S, Ito M, Morinaga S, Kudoh H (2016) **From**
833 **the laboratory to the field: assaying histone methylation at *FLOWERING LOCUS C***
834 **in naturally growing *Arabidopsis halleri***. *Genes Genet Syst* **91:** 15-26.
835 https://doi.org/10.1266/ggs.15-00071
836 Novillo F, Medina J, Salinas J (2007) ***Arabidopsis* CBF1 and CBF3 have a different function**
837 **than CBF2 in cold acclimation and define different gene classes in the CBF regulon**.
838 *Proc Natl Acad Sci U S A* **104:** 21002-21007. https://doi.org/10.1073/pnas.0705639105
839 O'Malley RC, Huang SC, Song L, Lewsey MG, Bartlett A, Nery JR, Galli M, Gallavotti A, Ecker
840 JR (2016) **Cistrome and epicistrome features shape the regulatory DNA landscape**.
841 *Cell* **165:** 1280-1292. https://doi.org/10.1016/j.cell.2016.04.038
842 Park J, Lim CJ, Shen M, Park HJ, Cha JY, Iniesto E, Rubio V, Mengiste T, Zhu JK, Bressan RA,
843 Lee SY, Lee BH, Jin JB, Pardo JM, Kim WY, Yun DJ (2018) **Epigenetic switch from**
844 **repressive to permissive chromatin in response to cold stress**. *Proc Natl Acad Sci U S*
845 *A* **115:** E5400-E5409. https://doi.org/10.1073/pnas.1721241115

846 Park S, Gilmour SJ, Grumet R, Thomashow MF (2018) **CBF-dependent and CBF-independent**
847 **regulatory pathways contribute to the differences in freezing tolerance and cold-**
848 **regulated gene expression of two Arabidopsis ecotypes locally adapted to sites in**
849 **Sweden and Italy**. *PLoS One* **13:** e0207723.
850 https://doi.org/10.1371/journal.pone.0207723
851 Park S, Lee CM, Doherty CJ, Gilmour SJ, Kim Y, Thomashow MF (2015) **Regulation of the**
852 **Arabidopsis CBF regulon by a complex low-temperature regulatory network**. *Plant J*
853 **82:** 193-207. https://doi.org/10.1111/tpj.12796
854 Penfield S (2008) **Temperature perception and signal transduction in plants**. *New Phytol* **179:**
855 615-628. https://doi.org/10.1111/j.1469-8137.2008.02478.x
856 Qüesta JI, Song J, Geraldo N, An H, Dean C (2016) ***Arabidopsis* transcriptional repressor VAL1**
857 **triggers Polycomb silencing at *FLC* during vernalization**. *Science* **353:** 485-488.
858 https://doi.org/10.1126/science.aaf7354
859 Seo E, Lee H, Jeon J, Park H, Kim J, Noh YS, Lee I (2009) **Crosstalk between cold response and**
860 **flowering in *Arabidopsis* is mediated through the flowering-time gene *SOC1* and its**
861 **upstream negative regulator *FLC***. *Plant Cell* **21:** 3185-3197.
862 https://doi.org/10.1105/tpc.108.063883
863 Seo PJ, Park MJ, Lim MH, Kim SG, Lee M, Baldwin IT, Park CM (2012) **A self-regulatory circuit**
864 **of CIRCADIAN CLOCK-ASSOCIATED1 underlies the circadian clock regulation of**
865 **temperature responses in *Arabidopsis***. *Plant Cell* **24:** 2427-2442.
866 https://doi.org/10.1105/tpc.112.098723
867 Sheldon CC, Burn JE, Perez PP, Metzger J, Edwards JA, Peacock WJ, Dennis ES (1999) **The *FLF***
868 **MADS box gene: A repressor of flowering in Arabidopsis regulated by vernalization**
869 **and methylation**. *Plant Cell* **11:** 445-458. https://doi.org/10.1105/tpc.11.3.445
870 Sheldon CC, Rouse DT, Finnegan EJ, Peacock WJ, Dennis ES (2000) **The molecular basis of**
871 **vernalization: The central role of *FLOWERING LOCUS C* (*FLC*)**. *Proc Natl Acad Sci*
872 *U S A* **97:** 3753-3758. https://doi.org/10.1073/pnas.97.7.3753
873 Shi Y, Ding Y, Yang S (2018) **Molecular regulation of CBF signaling in cold acclimation**. *Trends*
874 *Plant Sci* **23:** 623-637. https://doi.org/10.1016/j.tplants.2018.04.002

875 Shindo C, Aranzana MJ, Lister C, Baxter C, Nicholls C, Nordborg M, Dean C (2005) **Role of
876 *FRIGIDA* and *FLOWERING LOCUS C* in determining variation in flowering time of
877 Arabidopsis**. *Plant Physiol* **138:** 1163-1173. https://doi.org/10.1104/pp.105.061309
878 Shinozaki K, Yamaguchi-Shinozaki K, Seki M (2003) **Regulatory network of gene expression
879 in the drought and cold stress responses**. *Curr Opin Plant Biol* **6:** 410-417.
880 https://doi.org/10.1016/s1369-5266(03)00092-x
881 Shu H, Nakamura M, Siretskiy A, Borghi L, Moraes I, Wildhaber T, Gruissem W, Hennig L (2014)
882 ***Arabidopsis* replacement histone variant H3.3 occupies promoters of regulated genes**.
883 *Genome Biol* **15:** R62. https://doi.org/10.1186/gb-2014-15-4-r62
884 Song Y, Zhang X, Li M, Yang H, Fu D, Lv J, Ding Y, Gong Z, Shi Y, Yang S (2021) **The direct
885 targets of CBFs: In cold stress response and beyond**. *J Integr Plant Biol* **63:** 1874-1887.
886 https://doi.org/10.1111/jipb.13161
887 Stockinger EJ, Gilmour SJ, Thomashow MF (1997) ***Arabidopsis thaliana CBF1* encodes an AP2
888 domain-containing transcriptional activator that binds to the C-repeat/DRE, a cis-
889 acting DNA regulatory element that stimulates transcription in response to low
890 temperature and water deficit**. *Proc Natl Acad Sci U S A* **94:** 1035-1040.
891 https://doi.org/10.1073/pnas.94.3.1035
892 Sung S, Amasino RM (2004a) **Vernalization and epigenetics: how plants remember winter**.
893 *Curr Opin Plant Biol* **7:** 4-10. https://doi.org/10.1016/j.pbi.2003.11.010
894 Sung S, Amasino RM (2004b) **Vernalization in *Arabidopsis thaliana* is mediated by the PHD
895 finger protein VIN3**. *Nature* **427:** 159-164. https://doi.org/10.1038/nature02195
896 Sung S, He Y, Eshoo TW, Tamada Y, Jonson L, Nakahigashi K, Goto K, Jacobsen SE, Amasino
897 RM (2006) **Epigenetic maintenance of the vernalized state in Arabidopsis thaliana
898 requires LIKE HETEROCHROMATIN PROTEIN 1**. *Nat Genet* **38:** 706-710.
899 https://doi.org/10.1038/ng1795
900 Swiezewski S, Liu F, Magusin A, Dean C (2009) **Cold-induced silencing by long antisense
901 transcripts of an *Arabidopsis* Polycomb target**. *Nature* **462:** 799-802.
902 https://doi.org/10.1038/nature08618
903 Thomashow MF (1999) **PLANT COLD ACCLIMATION: Freezing tolerance genes and**

904 **regulatory mechanisms**. *Annu Rev Plant Physiol Plant Mol Biol* **50:** 571-599.
905 https://doi.org/10.1146/annurev.arplant.50.1.571
906 Thomashow MF (2010) **Molecular basis of plant cold acclimation: Insights gained from**
907 **studying the CBF cold response pathway**. *Plant Physiol* **154:** 571-577.
908 https://doi.org/10.1104/pp.110.161794
909 Thomashow MF, Stockinger EJ, Jaglo-Ottosen KR, Gilmour SJ, Zarka DG (1997) **Function and**
910 **regulation of *Arabidopsis thaliana COR* (cold-regulated) genes**. *Acta Physiol Plant* **19:**
911 497-504. https://doi.org/10.1007/s11738-997-0046-1
912 Wang ZW, Wu Z, Raitskin O, Sun Q, Dean C (2014) **Antisense-mediated *FLC* transcriptional**
913 **repression requires the P-TEFb transcription elongation factor**. *Proc Natl Acad Sci U*
914 *S A* **111:** 7468-7473. https://doi.org/10.1073/pnas.1406635111
915 Weiser CJ (1970) **Cold resistance and injury in woody plants: Knowledge of hardy plant**
916 **adaptations to freezing stress may help us to reduce winter damage**. *Science* **169:** 1269-
917 1278. https://doi.org/10.1126/science.169.3952.1269
918 Went FW (1953) **The effect of temperature on plant growth**. *Annu Rev Plant Phys* **4:** 347-362.
919 https://doi.org/10.1146/annurev.pp.04.060153.002023
920 Wood CC, Robertson M, Tanner G, Peacock WJ, Dennis ES, Helliwell CA (2006) **The *Arabidopsis***
921 ***thaliana* vernalization response requires a polycomb-like protein complex that also**
922 **includes VERNALIZATION INSENSITIVE 3**. *Proc Natl Acad Sci U S A* **103:** 14631-
923 14636. https://doi.org/10.1073/pnas.0606385103
924 Wu Z, Fang X, Zhu D, Dean C (2020) **Autonomous pathway: *FLOWERING LOCUS C***
925 **repression through an antisense-mediated chromatin-silencing mechanism**. *Plant*
926 *Physiol* **182:** 27-37. https://doi.org/10.1104/pp.19.01009
927 Xu C, Fang X, Lu T, Dean C (2021) **Antagonistic cotranscriptional regulation through**
928 **ARGONAUTE1 and the THO/TREX complex orchestrates *FLC* transcriptional**
929 **output**. *Proc Natl Acad Sci U S A* **118**. https://doi.org/10.1073/pnas.2113757118
930 Xu C, Wu Z, Duan HC, Fang X, Jia G, Dean C (2021) **R-loop resolution promotes co-**
931 **transcriptional chromatin silencing**. *Nat Commun* **12:** 1790.
932 https://doi.org/10.1038/s41467-021-22083-6

933 Yang H, Berry S, Olsson TSG, Hartley M, Howard M, Dean C (2017) **Distinct phases of**
934 **Polycomb silencing to hold epigenetic memory of cold in *Arabidopsis***. *Science* **357:**
935 1142-1145. https://doi.org/10.1126/science.aan1121
936 Yang H, Howard M, Dean C (2014) **Antagonistic roles for H3K36me3 and H3K27me3 in the**
937 **cold-induced epigenetic switch at *Arabidopsis FLC***. *Curr Biol* **24:** 1793-1797.
938 https://doi.org/10.1016/j.cub.2014.06.047
939 Yoo SD, Cho YH, Sheen J (2007) ***Arabidopsis* mesophyll protoplasts: a versatile cell system for**
940 **transient gene expression analysis**. *Nat Protoc* **2:** 1565-1572.
941 https://doi.org/10.1038/nprot.2007.199
942 Yuan W, Luo X, Li Z, Yang W, Wang Y, Liu R, Du J, He Y (2016) **A *cis* cold memory element**
943 **and a *trans* epigenome reader mediate Polycomb silencing of *FLC* by vernalization in**
944 ***Arabidopsis***. *Nat Genet* **48:** 1527-1534. https://doi.org/10.1038/ng.3712
945 Zhao C, Zhang Z, Xie S, Si T, Li Y, Zhu JK (2016) **Mutational evidence for the critical role of**
946 **CBF transcription factors in cold acclimation in Arabidopsis**. *Plant Physiol* **171:** 2744-
947 2759. https://doi.org/10.1104/pp.16.00533
948 Zhao Y, Antoniou-Kourounioti RL, Calder G, Dean C, Howard M (2020) **Temperature-**
949 **dependent growth contributes to long-term cold sensing**. *Nature* **583:** 825-829.
950 https://doi.org/10.1038/s41586-020-2485-4
951 Zhao Y, Zhu P, Hepworth J, Bloomer R, Antoniou-Kourounioti RL, Doughty J, Heckmann A, Xu
952 C, Yang H, Dean C (2021) **Natural temperature fluctuations promote *COOLAIR***
953 **regulation of *FLC***. *Genes Dev* **35:** 888-898. https://doi.org/10.1101/gad.348362.121
954 Zhu P, Lister C, Dean C (2021) **Cold-induced *Arabidopsis* FRIGIDA nuclear condensates for**
955 ***FLC* repression**. *Nature* **599:** 657-661. https://doi.org/10.1038/s41586-021-04062-5

Figures

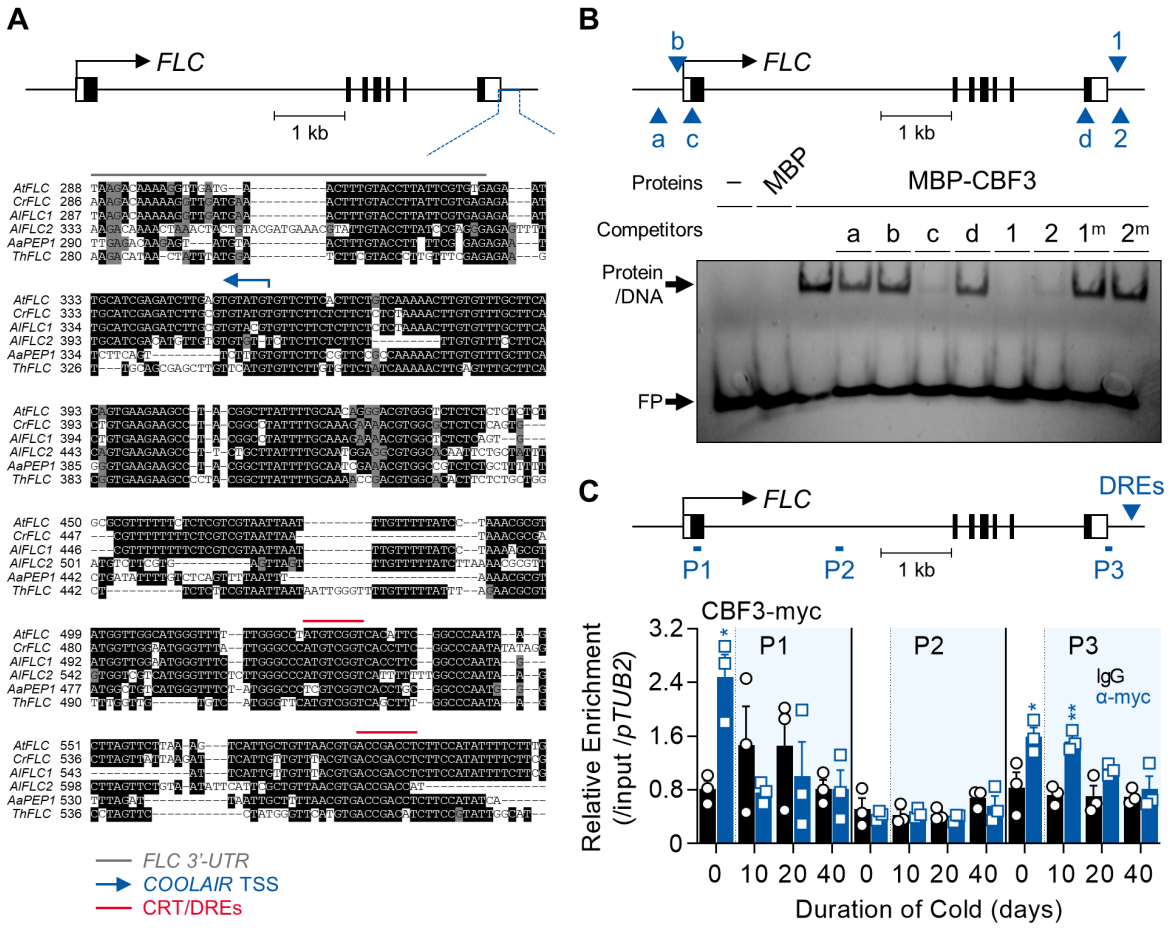

Figure 1. CBF3 directly binds to the CRT/DREs at the 3′-end of *FLC*.

(A) Comparison of sequences around the 3′-end of the *FLC* orthologs from Arabidopsis relatives. The upper graphic presents the gene structure of *AtFLC*. The black boxes, black lines, and white boxes indicate exons, introns, and UTRs, respectively. The blue line presents the region used for sequence comparison among six orthologous genes from five plant species. In the sequence alignment below, the grey line indicates the 3′-UTR of *FLC* orthologs, the blue arrow indicates the

965 transcriptional start site of *AtCOOLAIR*, and the red lines indicate CRT/DREs. At, *Arabidopsis*
966 *thaliana*; Cr, *Capsella rubella*; Al, *Arabidopsis lyrata*; Aa, *Arabis alpina*; Th, *Thellungiella*
967 *halophila*.
968 **(B)** EMSA using one of the CRT/DREs located at the *COOLAIR* promoter, DRE1, as a probe. In
969 the upper graphic showing *AtFLC* gene structure, CRT/DRE-like sequences are marked as blue
970 arrows and labelled as a, b, c, and d for CRT/DRE-like sequences and as 1 and 2 for CRT/DRE
971 sequences. For the competition assay, these CRT/DRE-like sequences and mutant forms of DRE1
972 and DRE2 were used as competitors. A 100-fold molar excess of unlabelled competitors was added.
973 No protein (−) or maltose binding protein (MBP) were used as controls. FP, free probe.
974 **(C)** ChIP assay result showing the enrichment of CBF3-myc protein on the *AtFLC* locus. Samples
975 of NV, 10V, 20V, and 40V plants of *pSuper:CBF3-myc* were collected at zeitgeber time (ZT) 4 in
976 an SD cycle. The CBF3-chromatin complex was immunoprecipitated (IP) with anti-myc
977 antibodies (blue bars), and mouse IgG (black bars) was used as a control. Positions of qPCR
978 amplicons used for ChIP-qPCR analysis are illustrated as P1, P2, and P3 in the upper graphic. The
979 blue arrows in the graphic denote the position of CRT/DREs and CRT/DRE-like sequences located
980 on the *FLC* gene. ChIP-qPCR results have been represented as mean ± SEM of the three biological
981 replicates in the lower panel. Open circles and squares represent each data-point. Relative
982 enrichments of the IP/5% input were normalized to that of *pTUB2*. The blue shading indicates the
983 cold period. Asterisks indicate a significant difference between IgG and anti-myc ChIP-qPCR
984 results at each vernalization time-point (*, $P < 0.05$; **, $P < 0.01$; unpaired Student's *t*-test).
985
986 **Figure 1—figure supplement 1.** CBF proteins directly bind to the sequence at the 3′-end of *FLC*

987 in DNA affinity purification sequencing (DAP-seq).

988 **Figure 1—figure supplement 2.** CBF3 binds to DRE1 and DRE2 on the *COOLAIR* promoter and

989 DREc on the first exon of *FLC.*

990 **Figure 1—source data 1.** Uncropped labelled gel image and the original image file for the EMSA

991 result.

992 **Figure 1—figure supplement 2—source data 1.** Uncropped labelled gel images and the original

993 image files for the EMSA results.

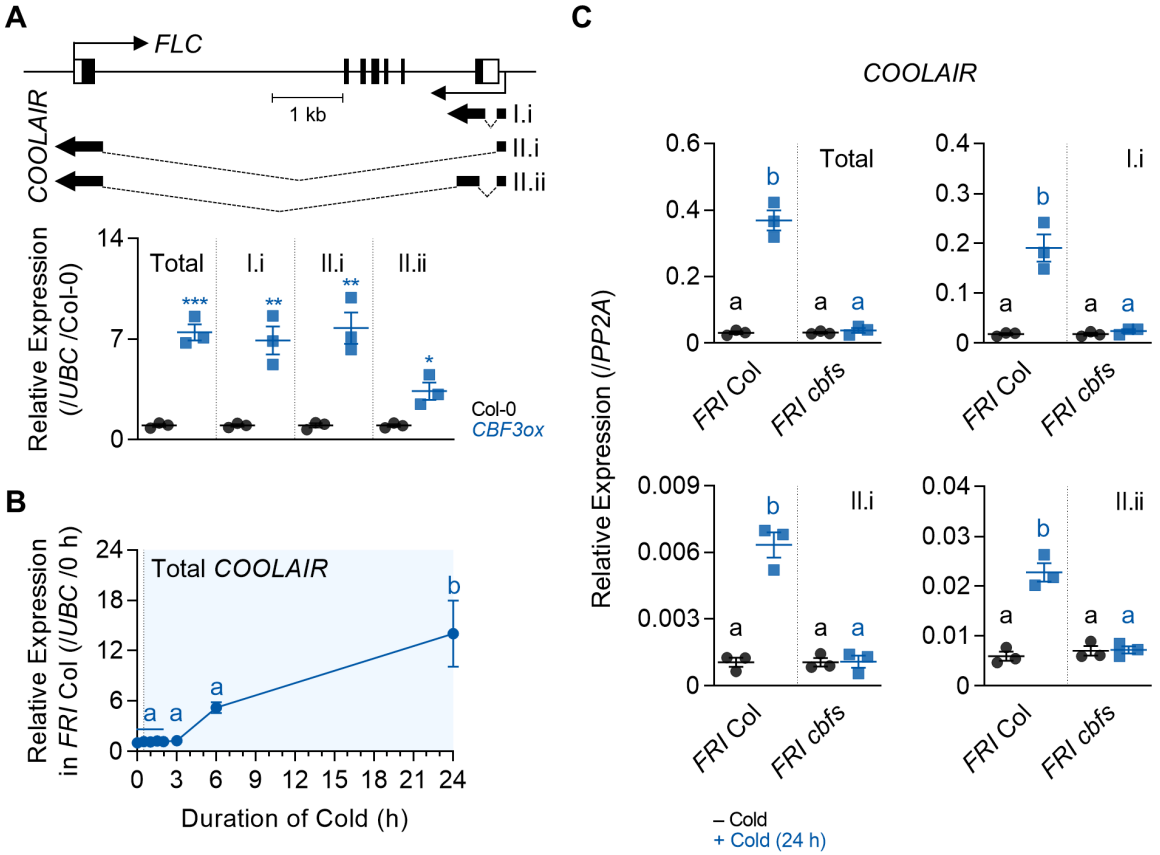

994

995 **Figure 2. *COOLAIR* shows a similar expression pattern with CBF regulons.**

996 **(A)** Expression levels of total *COOLAIR* and *COOLAIR* isoforms in the wild-type (Col-0) and
997 *CBF3*-overexpressing plants (*pSuper:CBF3-myc*). The gene structures of *FLC* and *COOLAIR*
998 variants are illustrated in the upper panel. The thin black arrows indicate the transcription start
999 sites of *FLC* and *COOLAIR*. The thick black arrows indicate the exons of each *COOLAIR* isoform.
1000 The structures of proximal (I.i) and distal (II.i and II.ii) *COOLAIR* isoforms are shown. The primer
1001 sets used for total, proximal (I.i), and distal (II.i, II.ii) *COOLAIR*s are marked in ***Figure 2—figure***
1002 ***supplement 1***. Relative transcript levels of total *COOLAIR* and *COOLAIR* variants were
1003 normalized to that of *UBC* and have been represented as mean ± SEM of three biological replicates.

1004 Dots and squares represent each data-point. Asterisks indicate a significant difference as compared
1005 to the wild type (*, $P < 0.05$; **, $P < 0.01$; ***, $P < 0.001$; unpaired Student's *t*-test).
1006 **(B)** Expression dynamics of total *COOLAIR* after short-term cold (0, 0.5, 1, 1.5, 2, 3, 6, and 24 h)
1007 treatment. Wild types (*FRI* Col) were subjected to 4°C cold and harvested at each time-point.
1008 Relative transcript levels of total *COOLAIR* to *UBC* were normalized to that of non-cold treated
1009 wild type. The values have been represented as mean ± SEM of three biological replicates. The
1010 blue shading indicates periods under cold treatment. Significant differences have been marked
1011 using different letters (a, b; $P < 0.05$; one-way ANOVA followed by Tukey's post-hoc test).
1012 **(C)** Transcript levels of total *COOLAIR* and *COOLAIR* isoforms in wild type and *cbfs-1* mutant
1013 before (−Cold) and after (+Cold) a day of 4°C cold treatment. Relative levels of total *COOLAIR*
1014 and *COOLAIR* variants were normalized to that of *PP2A*. Values have been represented as
1015 mean ± SEM of three biological replicates. Dots and squares indicate each data-point. Significant
1016 differences have been marked using different letters (a, b; $P < 0.05$; two-way ANOVA followed by
1017 Tukey's post-hoc test).
1018
1019 **Figure 2—figure supplement 1.** Overexpression of *CBF1*, *2*, or *3* causes an increase in *COOLAIR*
1020 level, but the effects on *COOLAIR* variants are subtly different.

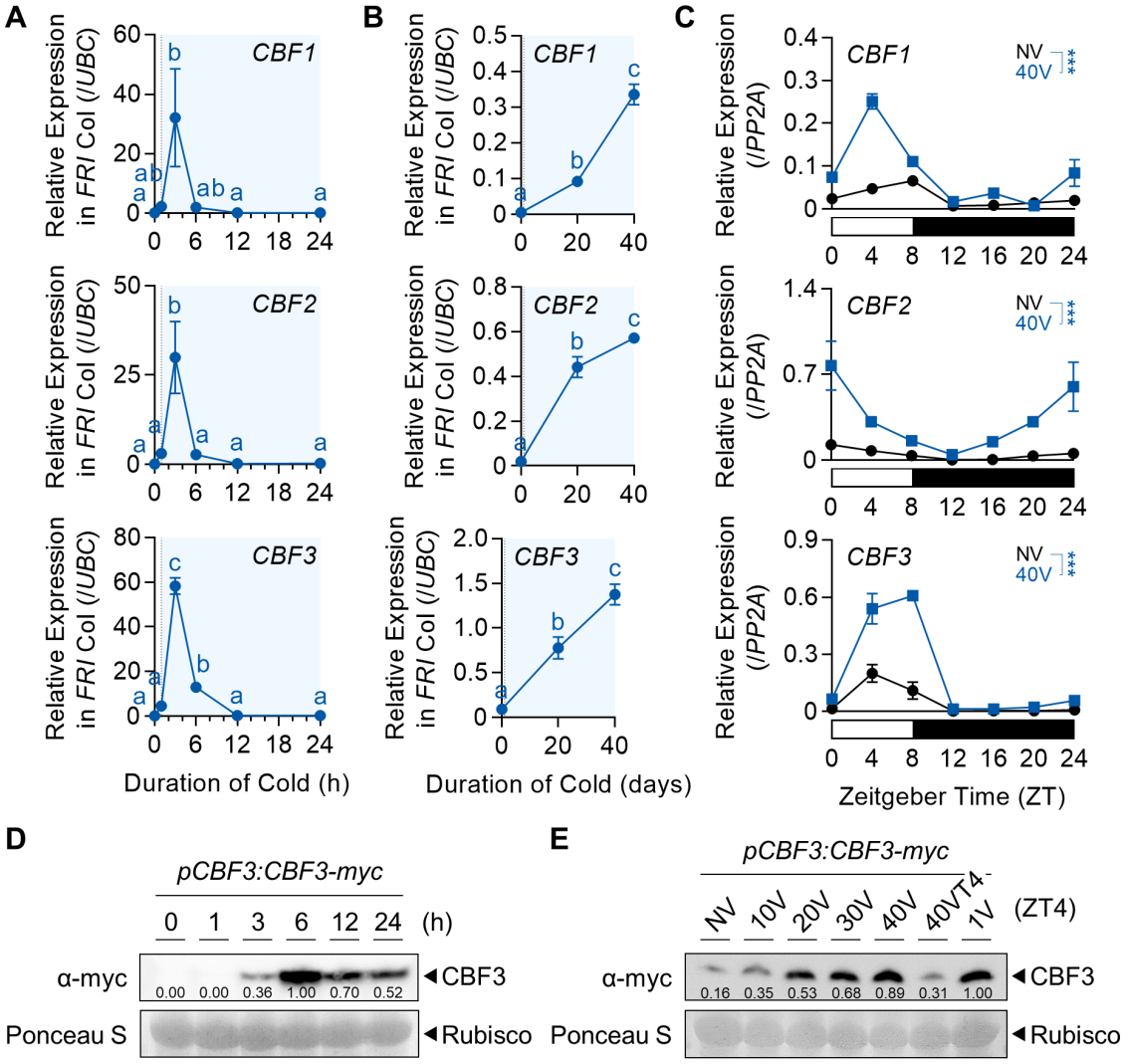

Figure 3. Protein levels of CBFs increase during the vernalization process.

(A) Transcript levels of *CBF1*, *2*, and *3* under short-term cold exposure. Wild-type plants were subjected to 0, 1, 3, 6, 12, and 24 h of 4°C cold treatment. Relative levels of *CBF1*, *2*, and *3* were normalized to that of *UBC*. Values have been represented as mean ± SEM of three biological replicates. The blue shadings indicate cold periods. Significant differences have been marked using different letters (a–c; $P < 0.05$; one-way ANOVA followed by Tukey's post-hoc test).

1028 **(B)** Transcript levels of *CBF1*, *2*, and *3* after 20V and 40V. Wild-type plants were treated with 4°C
1029 vernalization under an SD cycle and collected at ZT4. Relative levels of *CBF1*, *2*, and *3* were
1030 normalized to that of *UBC*. Values have been represented as mean ± SEM of three biological
1031 replicates. The blue shadings denote periods under cold. Significant differences have been marked
1032 using different letters (a–c; $P < 0.05$; one-way ANOVA followed by Tukey's post-hoc test).
1033 **(C)** Daily rhythms of *CBF1*, *2*, and *3* transcript levels in NV or 40V plants. Col-0 plants grown
1034 under an SD cycle were collected every 4 h between ZT0 and ZT24. Relative transcript levels of
1035 *CBF1*, *2*, and *3* were normalized to that of *PP2A*. Values have been represented as mean ± SEM of
1036 three biological replicates. The white and black bars represent light and dark periods, respectively.
1037 Asterisks indicate a significant difference between NV and 40V (***, $P < 0.001$; two-way
1038 ANOVA).
1039 **(D)** Dynamics of CBF3 protein level under short-term cold exposure. The *pCBF3:CBF3-myc*
1040 transgenic plants were subjected to 0, 1, 3, 6, 12, and 24 h of 4°C cold treatment. CBF3 proteins
1041 were detected using anti-myc antibodies. Rubisco was considered the loading control. Numbers
1042 below each band indicate relative signal intensity compared to 6 h. The mean values of two
1043 biological replicates are presented.
1044 **(E)** Increase of CBF3 protein level during the vernalization process. The *pCBF3:CBF3-myc*
1045 transgenic plants, subjected to 4°C vernalization, were collected at ZT4 of the indicated time-point.
1046 CBF3 proteins were detected using anti-myc antibodies. Rubisco was considered the loading
1047 control. Numbers below each band indicate relative signal intensity compared to 1V. The mean
1048 values of three biological replicates are presented.
1049

1050 **Figure 3—figure supplement 1.** Vernalization increases CBF3 protein levels with a minor effect
1051 on the daily rhythm.
1052 **Figure 3—source data 1.** Uncropped labelled blot images and the original image files for the
1053 immunoblots.
1054 **Figure 3—figure supplement 1—source data 1.** Uncropped labelled blot images and the original
1055 image files for the immunoblots.

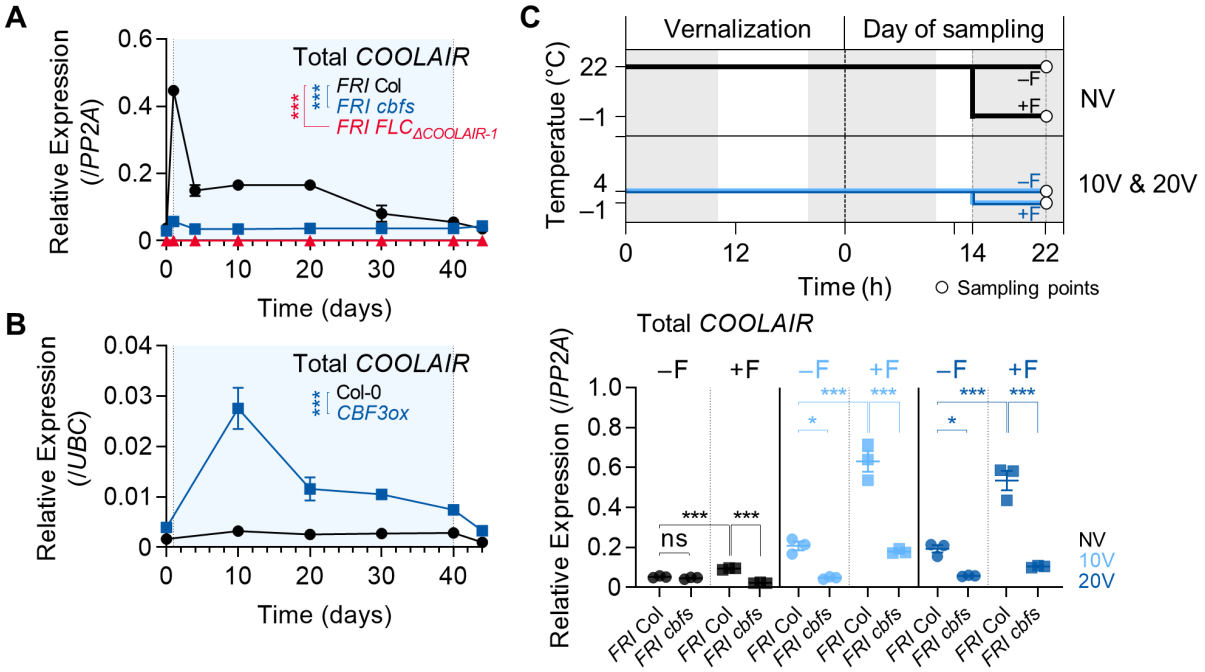

Figure 4. *CBF*s are involved in vernalization-induced *COOLAIR* expression.

(A) Expression dynamics of total *COOLAIR* in the wild-type, *cbfs-1*, and $FLC_{\Delta COOLAIR\text{-}1}$ plants during vernalization. Relative transcript levels of total *COOLAIR* were normalized to that of *PP2A*. Values have been represented as mean ± SEM of three biological replicates. Asterisks indicate a significant difference compared to the wild-type (***, $P < 0.001$; two-way ANOVA followed by Tukey's post-hoc test).

(B) Transcript level of total *COOLAIR* in wild-type (Col-0) and *CBF3*-overexpressing transgenic plant (*CBF3ox; pSuper:CBF3-myc*) during vernalization. Relative levels of total *COOLAIR* were normalized to that of *PP2A*. Values have been represented as mean ± SEM of three biological replicates. Asterisks indicate a significant difference between the wild-type and *CBF3* overexpressor (***, $P < 0.001$; two-way ANOVA). Blue shading denotes cold periods in (A) and

1068 (B).

1069 **(C)** Effect of first frost-mimicking treatment (8 h of freezing [< 0°C]) on the level of total
1070 *COOLAIR* in NV, 10V, and 20V wild type and *cbfs-1*. The upper panel shows a schematic of the
1071 experimental procedure. The non-frost treated (−F) wild type and *cbfs-1* were collected at ZT22
1072 after an 8 h of dark treatment at 22°C (NV) or 4°C (10V and 20V). For the first frost treatment,
1073 wild type and *cbfs-1* mutant were treated with an additional 8 h of −1°C (+F) under dark, and then
1074 the whole seedlings were collected at ZT22 for analysis. All the plants were grown under an SD
1075 cycle. The grey shadings denote dark periods. Total *COOLAIR* levels have been represented as
1076 mean ± SEM of three biological replicates in the lower panel. Dots and squares indicate each data-
1077 point. Relative levels of total *COOLAIR* were normalized to that of *PP2A*. Asterisks indicate a
1078 significant difference (*, $P < 0.05$; ***, $P < 0.001$; two-way ANOVA followed by Tukey's post-
1079 hoc test). ns, not significant ($P \geq 0.05$).

1080

1081 **Figure 4—figure supplement 1.** CBF regulons show strongly reduced expression in *cbfs* mutants
1082 similar to *COOLAIR*.

1083 **Figure 4—figure supplement 2.** Cold-triggered *COOLAIR* expression is impaired in *cbfs* mutants
1084 in Col-0 and Sweden-ecotype background.

1085 **Figure 4—figure supplement 3.** Freezing temperature increases the levels of *CBFs*.

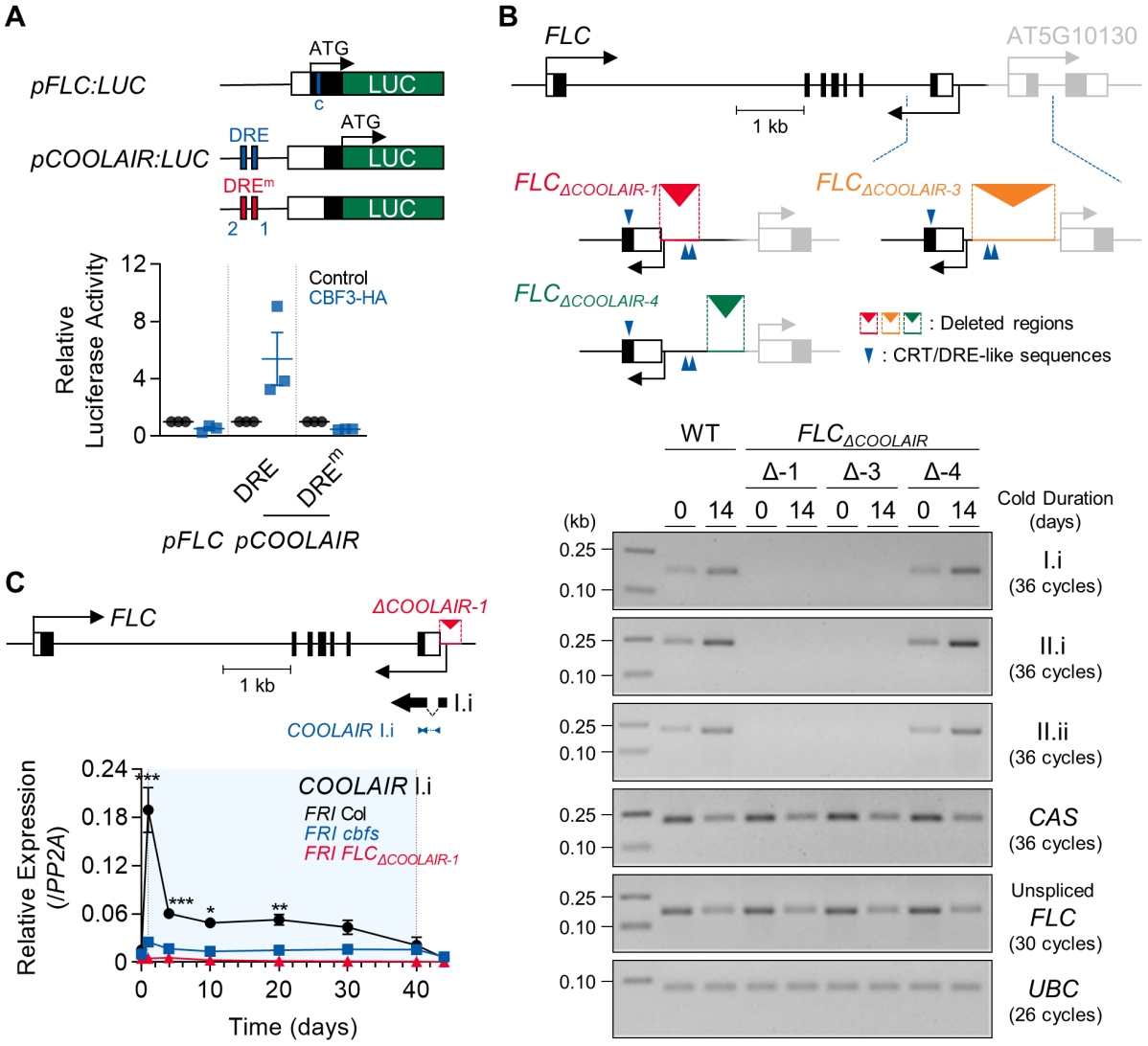

Figure 5. *COOLAIR* promoter region containing CRT/DREs is necessary for the *COOLAIR* induction by vernalization.

(A) Arabidopsis protoplast transfection assay showing that CBF3 activates *COOLAIR* promoter with wild-type CRT/DRE (DRE) but fails to activate the one with mutant CRT/DRE (DRE^m). A schematic of the reporter constructs used for the luciferase assay is presented in the upper panel. *pFLC:LUC* contains 1 kb of the promoter, the 5′-UTR, and the first exon of *FLC*. The blue line in

1093 the *pFLC:LUC* graphic indicates the location of DREc. Wild-type and mutant forms of
1094 *pCOOLAIR:LUC* include 1 kb of the *COOLAIR* promoter with the 3′-UTR and the last exon of
1095 *FLC*. The blue and red lines mark the positions of the wild-type (DRE) and mutant (DRE^m) forms
1096 of DRE1 and DRE2, respectively. Each reporter construct was co-transfected into Arabidopsis
1097 protoplast together with the *35S:CBF3-HA* effector construct. In parallel, *35S-NOS* plasmid was
1098 transfected as a control. The result is shown below. Relative luciferase activities were normalized
1099 to that of the *35S-NOS* control. Values have been represented as mean ± SEM of three biological
1100 replicates. Dots and squares represent each data-point.
1101 **(B)** Transcript levels of proximal (I.i) and distal (II.i and II.ii) *COOLAIR* isoforms in wild-type,
1102 $FLC_{\Delta COOLAIR\text{-}1}$, $FLC_{\Delta COOLAIR\text{-}3}$, and $FLC_{\Delta COOLAIR\text{-}4}$ plants before and after 14 days of vernalization.
1103 $FLC_{\Delta COOLAIR\text{-}1}$ and $FLC_{\Delta COOLAIR\text{-}3}$ have a 324- and 685-bp deletion of the *COOLAIR* promoter
1104 region, respectively, where DRE1 and 2 are located. $FLC_{\Delta COOLAIR\text{-}4}$ has a deletion in the 301-bp
1105 *COOLAIR* promoter region outside of DRE1 and -2 location. The positions of the deleted region
1106 are marked in red, orange, and green lines with reversed triangle in the upper graphic. Blue arrows
1107 denote CRT/DRE-like sequences. Black and grey bars denote exons, thin lines denote introns, and
1108 white bars denote UTRs of *FLC* and its neighboring gene (AT5G10130). Results of RT-PCR
1109 analysis are shown below. *UBC* was used as a quantitative control.
1110 **(C)** Transcript levels of proximal (I.i) *COOLAIR* isoform in wild-type, *cbfs-1*, and $FLC_{\Delta COOLAIR\text{-}1}$
1111 plants during vernalization. The position of the deleted region is marked in red lines with a reversed
1112 triangle in the upper graphic. Black bars denote exons, thin lines denote introns, and white bars
1113 denote UTRs of *FLC*. The thin black arrow below the gene structure indicates the transcriptional
1114 start site of *COOLAIR*. The thick black arrow below denotes exons of the type I.i *COOLAIR* variant.

1115 The position of the amplicon used for the qPCR analysis is marked with blue arrows. The result of
1116 qPCR analysis is presented in the lower panel. Relative transcript levels were normalized to that
1117 of *PP2A*. Values have been represented as mean ± SEM of three biological replicates. The blue
1118 shading indicates periods under cold treatment. Asterisks indicate a significant difference, as
1119 compared to NV (*, $P < 0.05$; **, $P < 0.01$; ***, $P < 0.001$; two-way ANOVA followed by Tukey's
1120 post-hoc test).
1121
1122 **Figure 5—figure supplement 1.** Genomic sequences near the deleted regions in two *COOLAIR*
1123 promoter deletion lines, $FLC_{\Delta COOLAIR\text{-}3}$ and $FLC_{\Delta COOLAIR\text{-}4}$.
1124 **Figure 5—figure supplement 2.** Proximal *COOLAIR* level is not significantly increased by *CBF3*
1125 overexpression in the $FLC_{\Delta COOLAIR}$ mutant lacking CRT/DREs.
1126 **Figure 5—source data 1.** Uncropped labelled gel images and the original image files for the RT-
1127 PCR results.

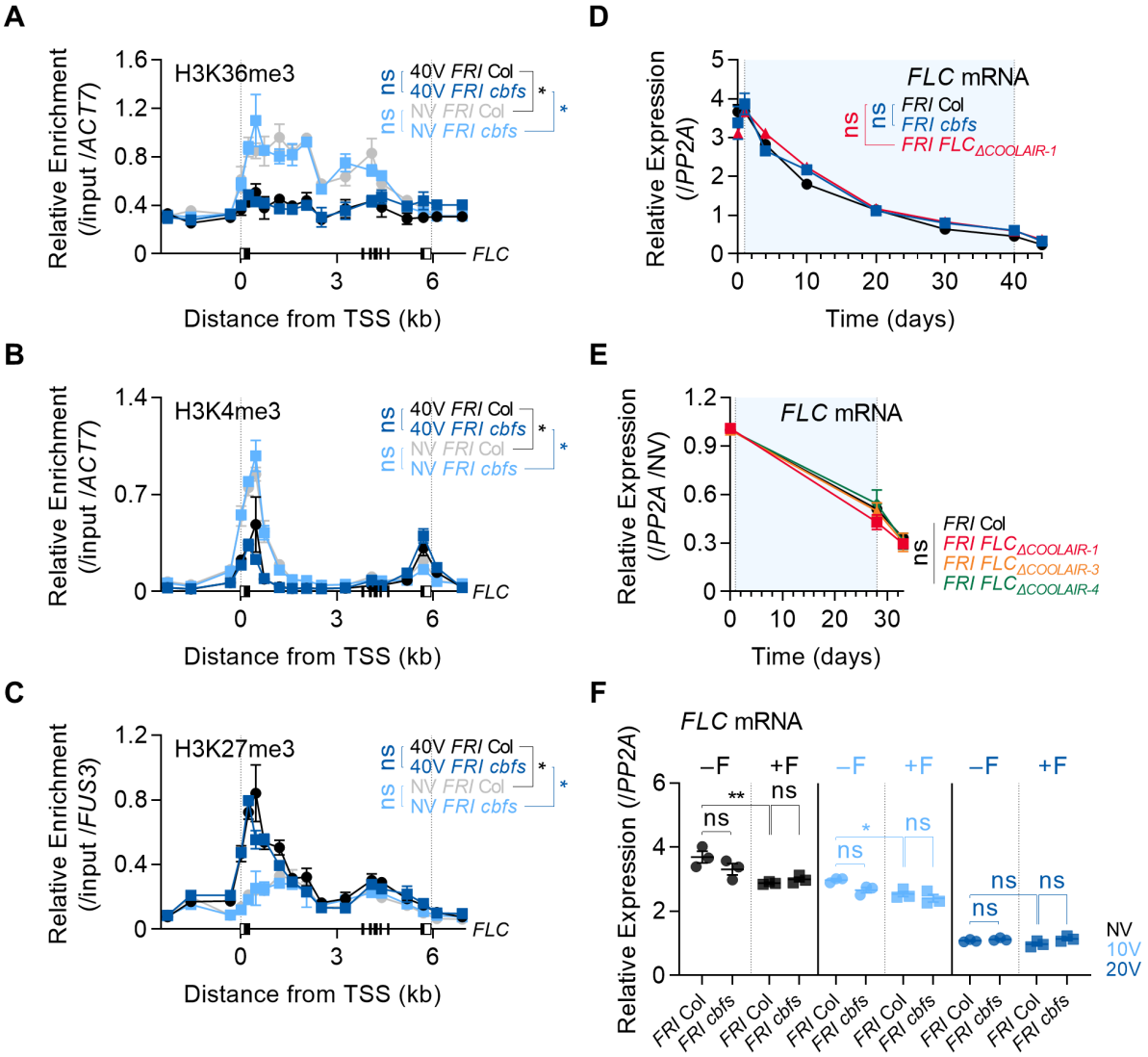

Figure 6. Vernalization-triggered epigenetic silencing of *FLC* is not affected by CBFs-mediated *COOLAIR* induction.

(A–C) Enrichments of H3K36me3 (A), H3K4me3 (B), and H3K27me3 (C) on the *FLC* locus in NV or 40V wild-type and *cbfs-1* plants. The whole seedlings were collected at ZT4 under an SD cycle. Modified histones were immunoprecipitated with anti-H3K36me3, anti-H3K4me3, or anti-H3K27me3 antibodies. H3K36me3, H3K4me3, and H3K27me3 enrichments of the IP/5% input

1135 were normalized to those of *ACT7* or *FUS3*. Relative enrichments have been represented as
1136 mean ± SEM of three biological replicates. One-way ANOVA and Tukey's post-hoc test were
1137 performed on the ChIP results obtained using two primer pairs corresponding to the *FLC*
1138 nucleation region (*Yang et al., 2017*). Asterisks indicate a significant difference (*, $P < 0.05$). ns,
1139 not significant ($P \geq 0.05$).

1140 **(D)** Transcript levels of *FLC* mRNA in wild-type, *cbfs-1* and $FLC_{\Delta COOLAIR\text{-}1}$ plants during and after
1141 vernalization. Blue shading denotes cold periods. Relative levels were normalized to that of *PP2A*.
1142 Values have been represented as mean ± SEM of three biological replicates. ns, not significant
1143 between wild type and mutants, as assessed using two-way ANOVA followed by Tukey's post-hoc
1144 test ($P \geq 0.05$).

1145 **(E)** Transcript levels of *FLC* mRNA in wild type, $FLC_{\Delta COOLAIR\text{-}1}$, $FLC_{\Delta COOLAIR\text{-}3}$, and $FLC_{\Delta COOLAIR\text{-}}$
1146 $_{4}$ during and after vernalization. Blue shading denotes cold periods. Relative levels were
1147 normalized to that of *PP2A*, and then normalized to NV of each genotype. Values have been
1148 represented as mean ± SEM of three biological replicates. ns, not significant between wild type
1149 and mutants, as assessed using two-way ANOVA followed by Tukey's post-hoc test ($P \geq 0.05$).

1150 **(F)** Effect of the first frost-mimicking treatment (8 h freezing) on the *FLC* mRNA level in wild
1151 type and *cbfs-1* after vernalization. NV, 10V, 20V, NV+F, 10V+F, and 20V+F plants were subjected
1152 to the treatments described in ***Figure 4C***. Relative levels were normalized to that of *PP2A*. Values
1153 have been represented as mean ± SEM of three biological replicates. Dots and triangles represent
1154 each data-point. Asterisks indicate a significant difference (*, $P < 0.05$; **, $P < 0.01$; two-way
1155 ANOVA followed by Tukey's post-hoc test). ns, not significant ($P \geq 0.05$).

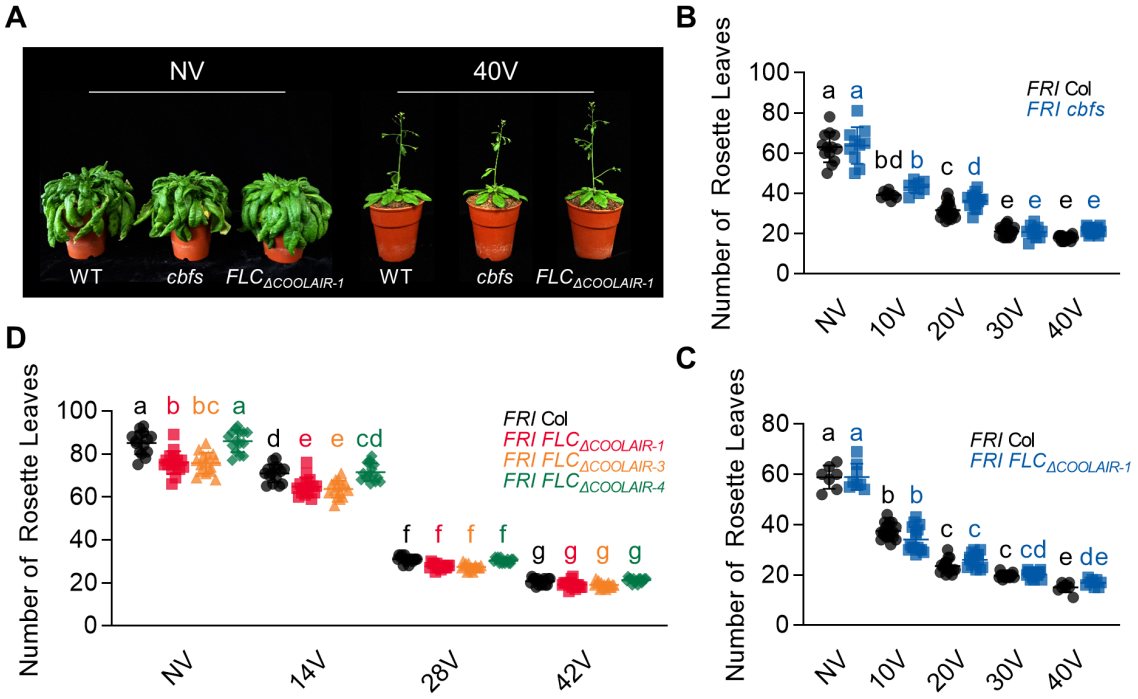

Figure 7. *CBF*-mediated *COOLAIR* induction under long-term cold is not absolutely necessary for vernalization response.

(A) Photographs of NV and 40V wild type, *cbfs-1*, and $FLC_{\Delta COOLAIR\text{-}1}$. NV plants were grown at 22°C under LD and 40V plants were grown at 22°C under LD after being treated for 40V under SD. The photos were taken when the NV plants started to bolt and the 40V plants showed the first open flower.

(B) Flowering times of NV and vernalized (10V–40V) wild type and *cbfs-1* plants. Flowering time was measured in terms of the number of rosette leaves produced when bolting. Plants were grown under LD after vernalization treatment. Bars and error bars represent the mean ± standard deviation (SD) of three biological replicates. Each dot and square indicate individual flowering time. Significant differences have been marked using different letters (a–e; two-way ANOVA followed

1168 by Tukey's post-hoc test; $P < 0.05$).

1169 **(C)** Flowering times of non-vernalized (NV) and vernalized (10V–40V) wild-type and
1170 $FLC_{\Delta COOLAIR}$ plants. Flowering time was measured in terms of the number of rosette leaves
1171 produced when bolting. Plants were grown under LD after vernalization. Bars and error bars
1172 indicate the mean ± SD. Each dot and square represent the individual flowering time. Significant
1173 differences have been indicated using different letters (a–e; two-way ANOVA followed by Tukey's
1174 post-hoc test; $P < 0.05$).

1175 **(D)** Flowering times of non-vernalized (NV) and vernalized (14V–42V) wild-type, $FLC_{\Delta COOLAIR-}$
1176 $_{1}$, $FLC_{\Delta COOLAIR-3}$, and $FLC_{\Delta COOLAIR-4}$ plants. Flowering time was measured in terms of the number
1177 of rosette leaves produced when bolting. Plants were grown under LD after vernalization. Bars
1178 and error bars indicate the mean ± SD. Each dot, square, triangle, and polygon represent the
1179 individual flowering time. Significant differences have been indicated using different letters (a–g;
1180 two-way ANOVA followed by Tukey's post-hoc test; $P < 0.05$).

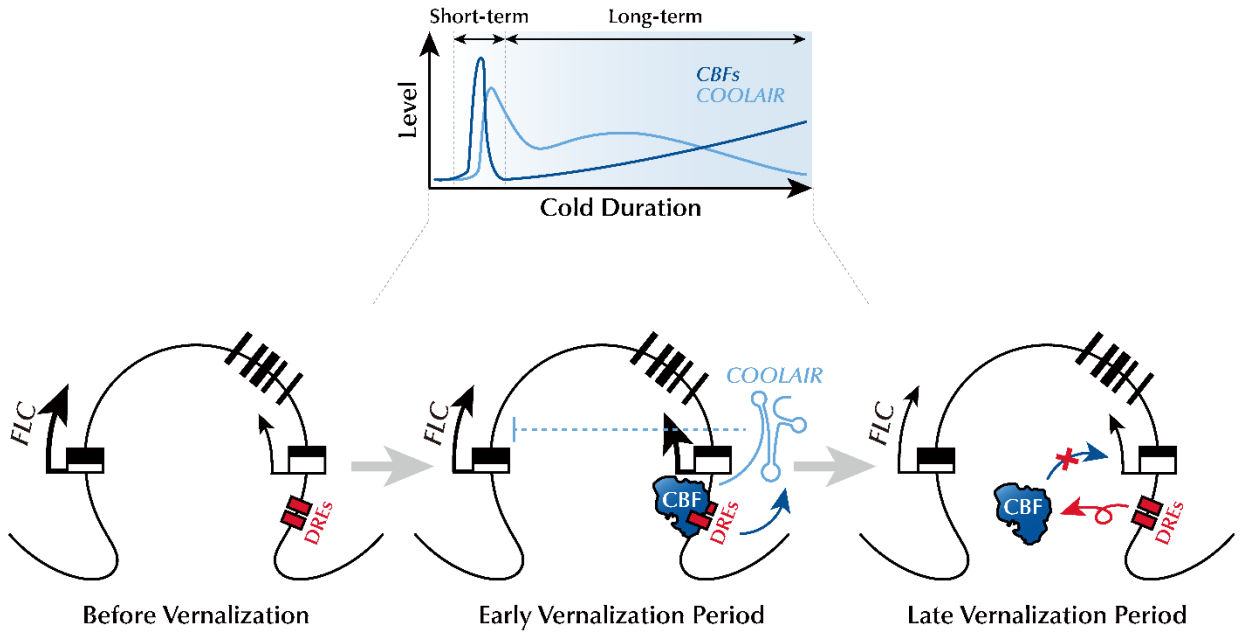

Figure 8. Schematic model describing the mechanism of CBFs-mediated *COOLAIR* expression during the early phase of vernalization.

During the early phase of vernalization, increased CBF upregulates *COOLAIR* expression by binding to CRT/DREs at the 3′-end of *FLC*. In the late phase of vernalization, owing to the silencing of *FLC* chromatin, CBF proteins are released from the CRT/DREs in the *COOLAIR* promoter, which leads to a reduction in *COOLAIR* levels.

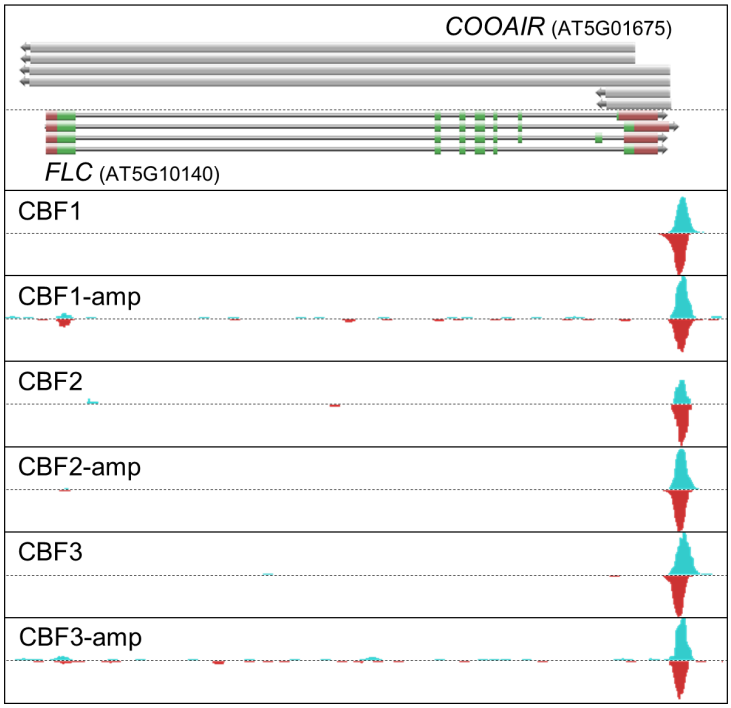

1188

1189 **Figure 1—figure supplement 1. CBF proteins directly bind to the sequence at the 3′-end of**

1190 ***FLC* in DNA affinity purification sequencing (DAP-seq).**

1191 DAP-seq results showed enrichment of CBF proteins at the *AtFLC* locus obtained from the Plant

1192 Cistrome Database (http://neomorph.salk.edu/dev/pages/shhuang/dap_web/pages/index.php;

1193 *O'Malley et al., 2016*). The top bars represent the transcribed regions of each *COOLAIR* variant.

1194 The bars below represent the structures of the alternatively spliced forms of the *FLC* transcript.

1195 The green, grey, and red bars indicate the exons, introns, and UTRs of *FLC*, respectively. The

1196 peaks below represent the positions of CBF enrichment. CBF-amp; amplification of DAP-seq

1197 results.

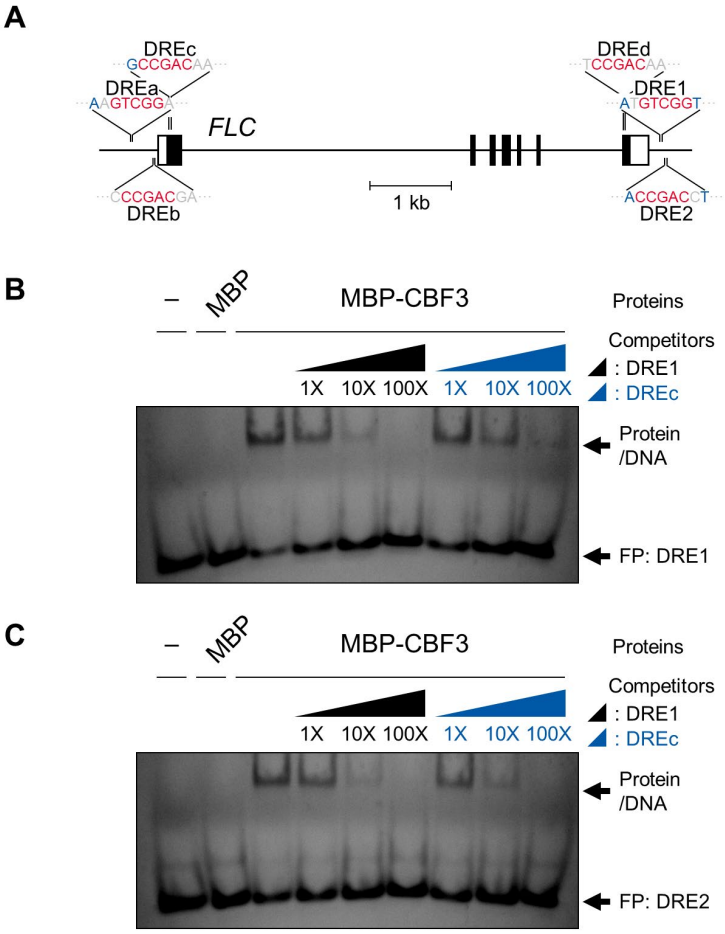

Figure 1—figure supplement 2. CBF3 binds to DRE1 and DRE2 on the *COOLAIR* promoter and DREc on the first exon of *FLC*.

(A) Schematic showing the positions of six CRT/DRE-like sequences distributed on the *AtFLC* locus. CRT/DRE sequences have been labelled as DRE1, 2, and CRT/DRE-like sequences have been labelled as DREa, b, c, and d. The black boxes, black lines, and white boxes represent exons, introns, and UTRs of *AtFLC*, respectively. The red bases indicate the core sequence (CCGAC) of CRT/DRE. The blue-colored bases represent bases known to determine the binding affinity of CBF3 to CRT/DRE (*Maruyama et al., 2004*).

1207 **(B–C)** EMSA using DRE1 (B) or DRE2 (C) as probe. For competition assay, DRE1, DRE2, and
1208 DREc were used as competitors. Molar excess (1-, 10-, and 100-fold) of unlabelled competitors
1209 was added. FP, free probe.

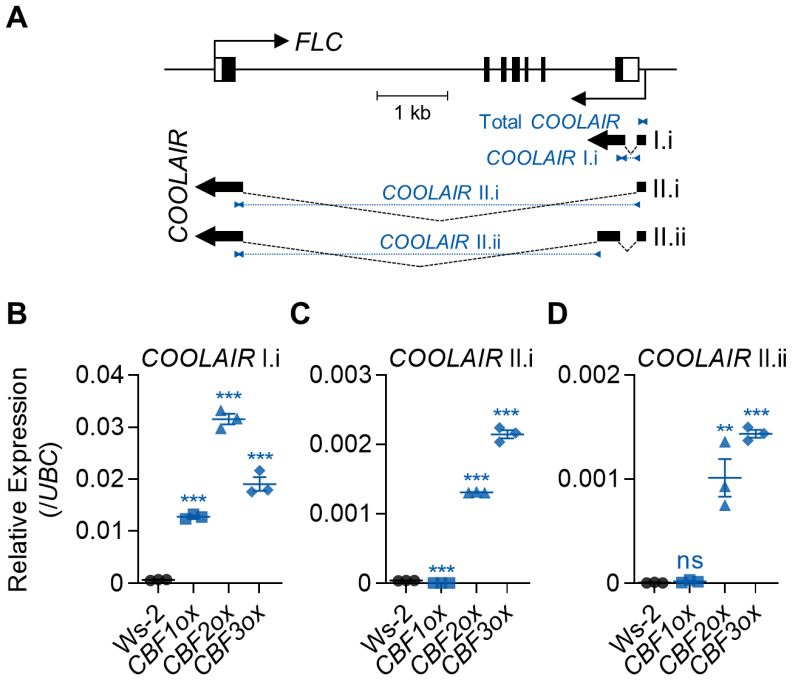

1210

1211 **Figure 2—figure supplement 1. Overexpression of *CBF1*, *2*, or *3* causes an increase in**

1212 ***COOLAIR* level, but the effects on *COOLAIR* variants are subtly different.**

1213 **(A)** Positions of qPCR amplicons used for detecting proximal (I.i) and distal (II.i and II.ii)

1214 *COOLAIR* variants. The black boxes denote exons, black lines denote introns, and white boxes

1215 denote UTRs of *FLC*. The thin black arrow below the gene structure indicates the transcription

1216 start site of *COOLAIR*. The thick black arrows below denote exons of type I.i, type II.i, and type

1217 II.ii *COOLAIR* variants. The positions of qPCR amplicons used for the qPCR analysis have been

1218 marked using blue arrow heads.

1219 **(B–D)** Transcript levels of *COOLAIR* variants in the wild type (Ws-2) and *CBF1*-, *2*-, and *3*-

1220 overexpressing transgenic plants (*35S:CBF1* [*CBF1ox*], *35S:CBF2* [*CBF2ox*], and *35S:CBF3*

1221 [*CBF3ox*], respectively; *Seo et al., 2009*). Relative levels of type I.i (B), type II.i (C), and type II.ii

1222 (D) *COOLAIR* were normalized to that of *UBC*. Values have been represented as mean ± SEM of
1223 three biological replicates. Dots, squares, triangles, and polygons represent each data-point.
1224 Asterisks indicate a significant difference, as compared to the wild type (**, $P < 0.01$; ***,
1225 $P < 0.001$; unpaired Student's *t*-test). ns, not significant ($P \geq 0.05$).

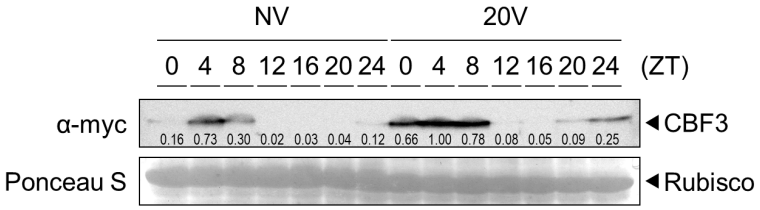

Figure 3—figure supplement 1. Vernalization increases CBF3 protein levels with a minor effect on the daily rhythm.

Daily rhythm of CBF3 protein level in NV or 20V plants. The *pCBF3:CBF3-myc* transgenic plants, subjected to 4°C vernalization, were collected every 4 h between ZT0 and ZT24. CBF3 protein was detected using anti-myc antibodies. Rubisco was used as loading control. The numbers below each band indicate the relative signal intensity compared to 20V ZT4. The mean values of three biological replicates are presented.

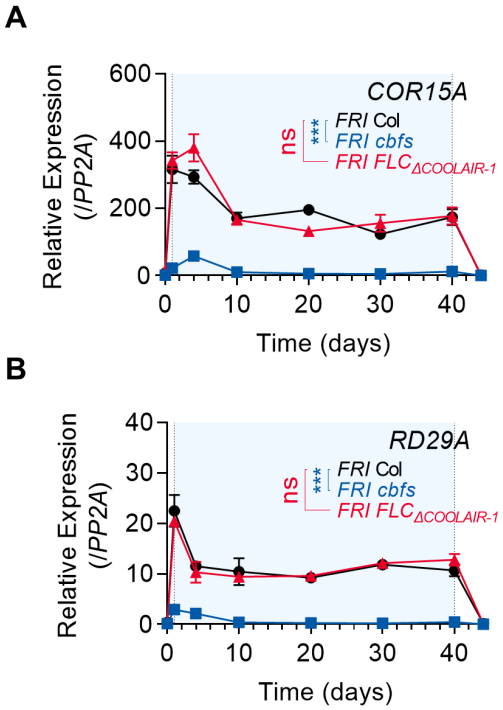

Figure 4—figure supplement 1. CBF regulons show strongly reduced expression in *cbfs* mutants similar to *COOLAIR*.

(A–B) Expression dynamics of *COR15A* (A) and *RD29A* (B) in the wild type, *cbfs-1*, and $FLC_{\Delta COOLAIR\text{-}1}$ plants during vernalization. Relative transcript levels of *COR15A* and *RD29A* were normalized to that of *PP2A*. Values have been represented as mean ± SEM of three biological replicates. Asterisks indicate a significant difference compared to the wild type (***, $P < 0.001$; two-way ANOVA followed by Tukey's post-hoc test). ns, not significant ($P \geq 0.05$). Blue shading denotes cold periods in (A) and (B).

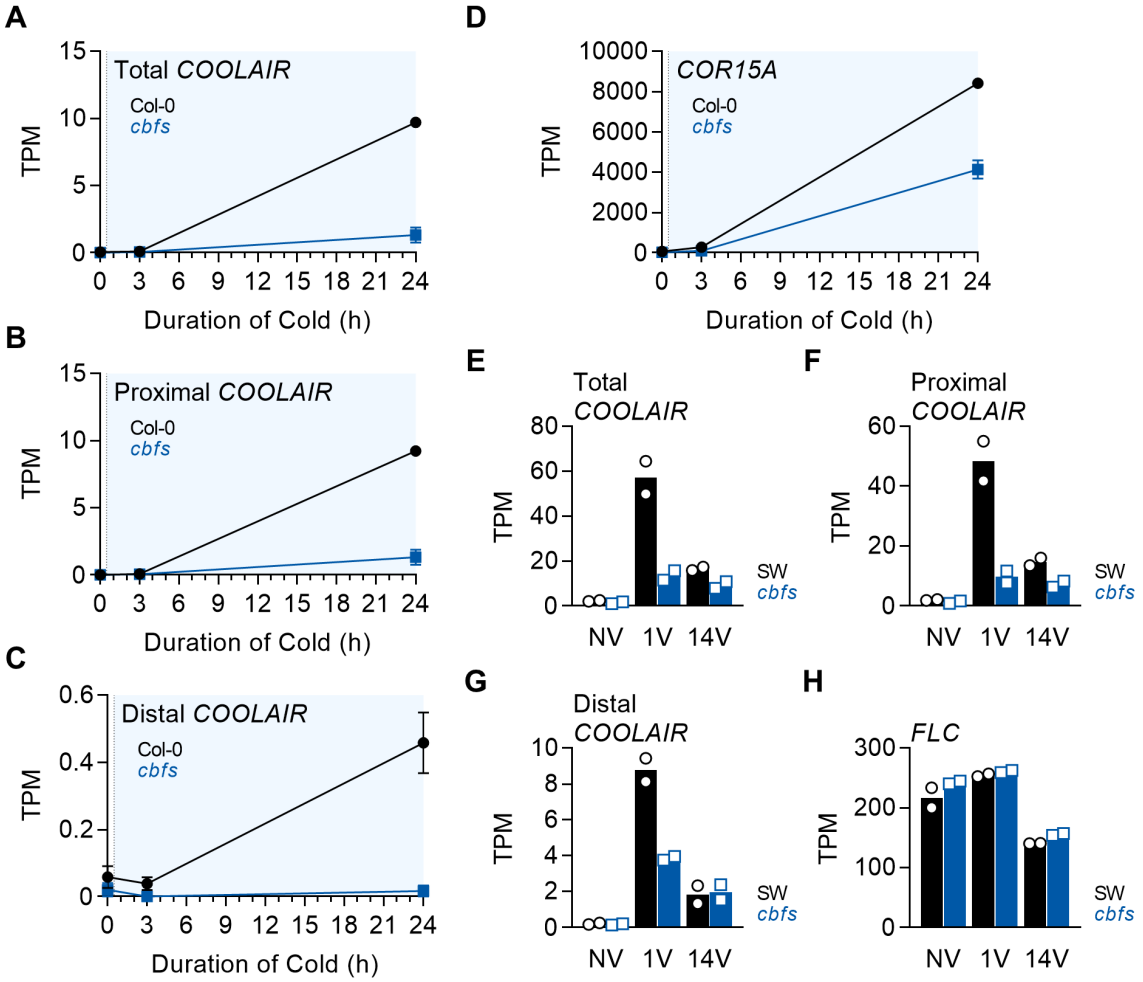

Figure 4—figure supplement 2. Cold-triggered *COOLAIR* expression is impaired in *cbfs* mutants in Col-0 and Sweden-ecotype background.

(A–D) Transcript levels of total (A), proximal (B), distal (C) *COOLAIR* and *COR15A* (D) in the wild type (Col-0) and *cbfs* mutant upon 0, 3, 24 h of cold exposure. The data were obtained from the analysis using RNA-seq data reported (*Zhao et al., 2016*). The mean values of transcript per million (TPM) of each gene obtained from three experimental replicates are shown. Error bars denote SEM.

1251 **(E–H)** Transcript levels of total (E), proximal (F), distal (G) *COOLAIR* and *FLC* (H) in NV, 1V,
1252 and 14V wild type (SW) and *cbfs* mutant. The data were obtained from the analysis using RNA-
1253 seq data reported (*S. Park et al., 2018*). SW, an Arabidopsis ecotype collected from Sweden. The
1254 mean values of the TPM of each gene obtained from two experimental replicates are shown. Open
1255 circles and squares represent each data-point.

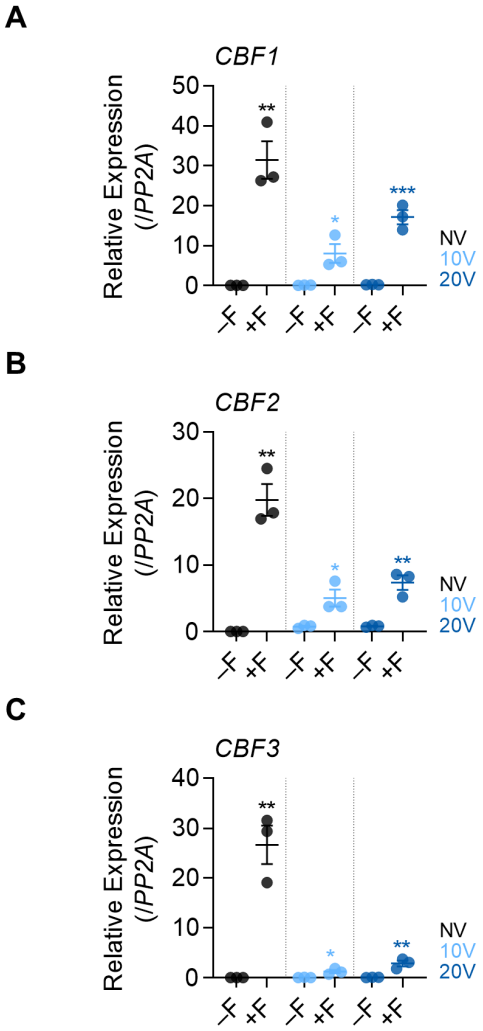

Figure 4—figure supplement 3. Freezing temperature increases the levels of *CBFs*.

(A–C) Effect of the first frost-mimicking treatment (8 h freezing) on the levels of *CBF1* (A), *2* (B), and *3* (C) in wild type after vernalization. NV, 10V, 20V, NV+F, 10V+F, and 20V+F plants were subjected to the treatments described in ***Figure 4C***. Relative levels were normalized to that of *PP2A*. Values have been represented as mean ± SEM of three biological replicates. Dots represent each data-point. Asterisks indicate a significant difference (*, $P < 0.05$; **, $P < 0.01$; ***, $P < 0.001$; unpaired Student's *t*-test).

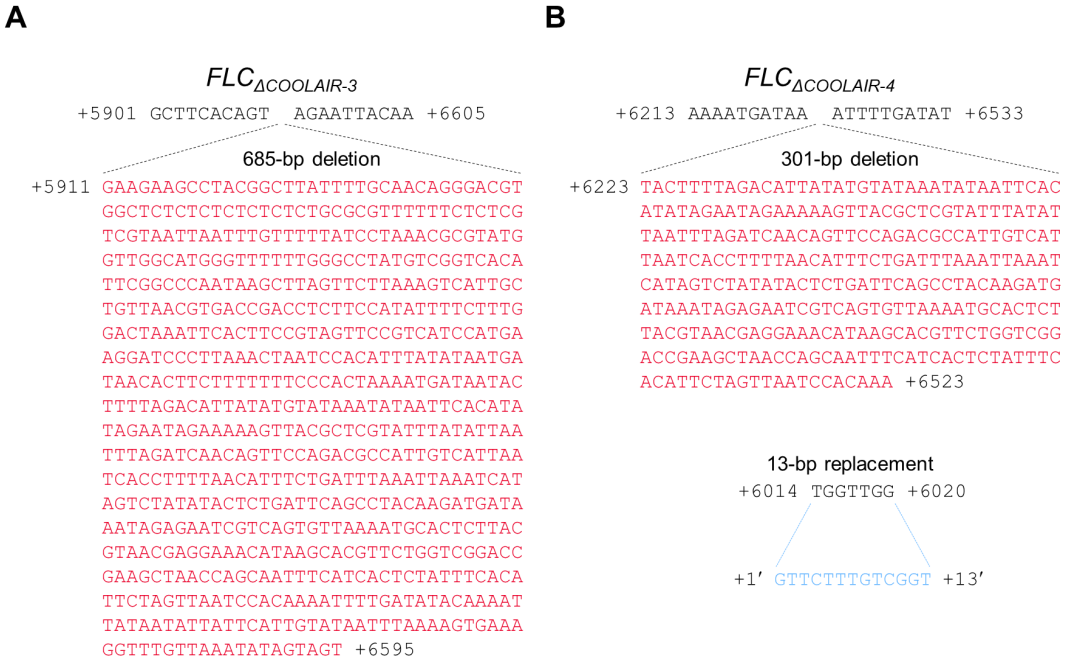

Figure 5—figure supplement 1. Genomic sequences near the deleted regions in two *COOLAIR* promoter deletion lines, *FLC*$_{\Delta COOLAIR\text{-}3}$ and *FLC*$_{\Delta COOLAIR\text{-}4}$.

(A–B) Genomic sequences around the deleted regions in newly generated *COOLAIR* promoter deletion lines, *FLC*$_{\Delta COOLAIR\text{-}3}$ (A) and *FLC*$_{\Delta COOLAIR\text{-}4}$ (B). Deleted or replaced sequences are marked in red and cyan, respectively.

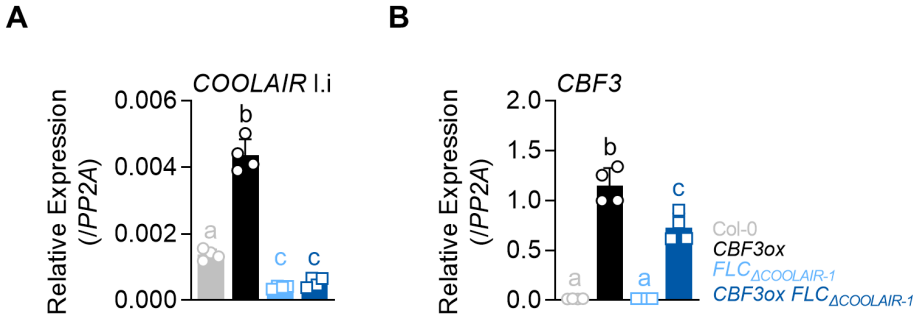

1270

1271 **Figure 5—figure supplement 2. Proximal *COOLAIR* level is not significantly increased by**

1272 ***CBF3* overexpression in the *FLC$_{\Delta COOLAIR}$* mutant lacking CRT/DREs.**

1273 **(A–B)** Expression levels of proximal *COOLAIR* variant I.i (A) and *CBF*3 (B) in non-vernalized

1274 wild type (Col-0), *pSuper:CBF3-myc* (*CBF3ox*), *FLC$_{\Delta COOLAIR\text{-}1}$*, and *pSuper:CBF3-myc*

1275 *FLC$_{\Delta COOLAIR\text{-}1}$* (*CBF3ox FLC$_{\Delta COOLAIR\text{-}1}$*). The whole seedlings were collected at 16 days after

1276 germination under an SD cycle. Relative levels were normalized to that of *PP2A*. Values have been

1277 represented as mean ± SD of four technical replicates from two biological replicates. Open circles

1278 and squares represent each data-point. Significant differences have been marked using different

1279 letters (a–c; $P < 0.05$; one-way ANOVA followed by Tukey's post-hoc test).